

Cosmological Non-Gaussianity from Neutrino Seesaw

Jingtao You,^a Linghao Song,^a Hong-Jian He,^{a,b} Chengcheng Han^c

^a*Tsung-Dao Lee Institute & School of Physics and Astronomy,
Key Laboratory for Particle Astrophysics and Cosmology,
Shanghai Key Laboratory for Particle Physics and Cosmology,
Shanghai Jiao Tong University, Shanghai, China*

^b*Department of Physics, Tsinghua University, Beijing, China;
Center for High Energy Physics, Peking University, Beijing, China*

^c*Department of Physics, Sun Yat-Sen University, Guangzhou 510275, China;
Key Laboratory for Particle Astrophysics and Cosmology,
Shanghai Jiao Tong University, Shanghai, China;
Asia Pacific Center for Theoretical Physics, Pohang 37673, Korea
E-mail: 119760616yjt@sjtu.edu.cn, lh.song@sjtu.edu.cn,
hjhe@sjtu.edu.cn, hanchch@mail.sysu.edu.cn*

ABSTRACT:

The neutrino mass generation via conventional seesaw mechanism is realized at high scales around $O(10^{14})\text{GeV}$, making the test of neutrino seesaw a great challenge. A striking fact is that the neutrino seesaw scale is typically around the cosmological inflation scale. In this work, we propose a framework incorporating inflation and neutrino seesaw in which the inflaton primarily decays into right-handed neutrinos after inflation. This decay process is governed by the inflaton interaction with the right-handed neutrinos that respects the shift symmetry. Through the neutrino seesaw mechanism, fluctuations of the Higgs field can modulate the inflaton decays, contributing to the curvature perturbation. We investigate the induced non-Gaussian signatures and demonstrate that such signatures provides an important means to probe the high-scale neutrino seesaw mechanism.

[arXiv:2412.16033]

Contents

1 Introduction	2
2 Dynamics of Higgs Field in the Early Universe	4
2.1 Dynamics of Higgs Field during Inflation	5
2.2 Evolution of Higgs Field after Inflation	8
3 Higgs Modulated Reheating Using Right-handed Neutrino	10
3.1 Model Realization and Setup	10
3.2 Higgs Modulated Reheating	13
4 Probing Neutrino Seesaw Using Primordial Non-Gaussianity	16
4.1 Analysis of Comoving Curvature Perturbation	16
4.2 Three-Point Correlation Function of Curvature Perturbation	18
4.3 Probing the Seesaw Scale through Local Non-Gaussianity	20
5 Conclusions	25
A Evolution of Higgs Field after Inflation	26
B Derivation of Non-Gaussianity	29
C Schwinger-Keldysh Propagators of Higgs Field	31
D Probability Distribution Function of Higgs Field	32
References	35

1 Introduction

The discovery of neutrino oscillations has pointed to tiny but nonzero neutrino masses of $O(0.1)\text{eV}$, which can be naturally generated by including the right-handed neutrinos within the structure of the Standard Model (SM) of particle physics. These right-handed neutrinos are the chiral partners of the left-handed neutrinos and they join together the Yukawa interactions with the Higgs doublet (just like any other leptons and quarks in the SM). But the right-handed neutrinos are pure singlets of the SM gauge group. As such they can naturally acquire large Majorana masses (M_R) and realize the seesaw mechanism [1][2] to naturally generate the tiny neutrino masses $m_\nu \sim v^2/M_R$, where $v = O(100)\text{GeV}$ denotes the vacuum expectation value of the SM Higgs doublet and the neutrino-Higgs Yukawa couplings are set to their natural values of $O(1)$. This generally predicts a high scale for neutrino seesaw, $M_R \sim v^2/m_\nu = O(10^{14})\text{GeV}$. Hence, given the current capabilities of

particle physics experiments, probing the neutrino seesaw mechanism at such high scales (M_R) poses a great challenge.

On the other hand, it is believed that the early universe underwent an inflationary epoch, during which the universe expanded exponentially over a very short period. Inflation not only resolves the flatness and horizon problems, but also seeds the primordial fluctuations that form the large-scale structure of the universe. The energy scale of inflation could be as high as $O(10^{14}\text{--}10^{16})$ GeV, characterized by the nearly constant Hubble parameter H_{inf} which is typically around 10^{14} GeV, providing an important window for probing new physics at high energy scales. It is intriguing to observe that both the neutrino seesaw and inflation can be realized around the same scale of $O(10^{14})$ GeV. In the minimal setup the inflation is triggered by a scalar inflaton field. The primordial fluctuations are generated by quantum fluctuations of the inflaton and can be directly measured through the Cosmic Microwave Background (CMB). The current CMB data indicate that these fluctuations are adiabatic and Gaussian [3–5].

However, inflation could also generate non-Gaussianity (NG) in the primordial perturbations [6][7], as characterized by n -point ($n \geq 3$) correlation functions of the comoving curvature perturbation ζ . The primordial non-Gaussianity can arise in models of multi-field inflation or single-field inflation with interactions, offering an ideal opportunity to probe the relevant new physics at high energy scales. One notable example is the “cosmological collider” method [8–11], which aims to explore high-scale particle physics by studying the non-Gaussian properties of large scale structures. Given the present non-observation of non-Gaussianity, the existing CMB measurements have already set constraints on the non-Gaussian parameter $f_{\text{NL}} \lesssim O(10)$ depending on the shapes considered. The future detection of the 21cm tomography could eventually reach the sensitivity down to the level of $f_{\text{NL}} \sim O(0.01)$ [12–14].

At the end of inflation, the inflaton would oscillate at the bottom of its potential and eventually transfer its energy to the SM particles, thereby reheats the universe. This sets the stage for the universe’s transition from the inflationary epoch to a radiation-dominated period, preceding the onset of Big Bang Nucleosynthesis (BBN). While observations of the large scale structures provide information about the inflation, details of the reheating process remain unclear. Since the right-handed neutrinos are singlets of the SM gauge group, it is fairly natural to expect that inflaton can couple directly to the right-handed neutrinos and predominantly decays into them after inflation. Then, these right-handed neutrinos could further decay into the SM particles through Yukawa interactions, and thus complete the reheating process. It is really appealing that this approach also naturally provides an initial setup for the leptogenesis [15], which generates sufficient right-handed neutrinos after reheating.

On the other hand, during inflation, not only does the inflaton fluctuate, but other light scalar fields also undergo fluctuations. In particular, the Higgs boson would acquire a field value near the Hubble scale, which varies across different horizon patches. This variation leads to discrimination on the right-handed neutrino masses in local regions of the universe via seesaw mechanism. In consequence, the inflaton’s decay rate into right-

handed neutrinos is modulated by the Higgs field value. This modulated reheating scenario provides a source of primordial curvature perturbations [16]. The associated non-Gaussian signatures open up a new window for probing the neutrino seesaw scale. We investigate in this work the effects of Higgs-modulated reheating and its potential to probe the high-scale neutrino seesaw mechanism. Moreover, this approach also provides a new framework of the cosmological Higgs collider (CHC), in which the Higgs modulated reheating is naturally realized by the inflaton decays into right-handed neutrinos within neutrino seesaw. Thus, particles which couples to the Higgs field would induce cosmological collider signatures, which we may call the neutrino-assisted cosmological Higgs collider (NCHC).¹

This paper is organized as follows. In Section 2, we discuss on the dynamics and evolution of the Higgs field during and after inflation. In Section 3, we present a minimal framework incorporating inflation and neutrino seesaw. Then, we analyze the curvature perturbations from the Higgs modulated reheating. In Section 4, we give the method to compute non-Gaussianity and present its numerical analysis. Finally, we conclude in Section 5. Appendices A-D provide the necessary formulas and technical derivations to support the analyses in the main text.

2 Dynamics of Higgs Field in the Early Universe

In this section, we discuss the physics with Higgs field during and after inflation. The Lagrangian density of the SM Higgs kinetic term and potential term is given by

$$\mathcal{L} = \sqrt{-g} \left[-g_{\mu\nu} D^\mu \mathbb{H}^\dagger D^\nu \mathbb{H} + \mu^2 \mathbb{H}^\dagger \mathbb{H} - \lambda (\mathbb{H}^\dagger \mathbb{H})^2 \right], \quad (2.1)$$

where \mathbb{H} is the SM Higgs doublet containing 4 independent scalar components. Note that the Higgs self-coupling might become negative at a scale around 10^{11} GeV depending on the precise value of the measured top quark mass [18]. Given that the Hubble parameter during inflation could be as high as 10^{14} GeV, the Higgs vacuum might become unstable during inflation. But the running of Higgs self-coupling is very sensitive to the measured top quark mass. Within the 3σ range of the current top mass measurement [19], it is still possible to keep the Higgs coupling positive and have a value of $O(0.001)$ at the inflation scale.²

In the following discussions, we denote the quantities at different epochs by using the corresponding subscripts, such as $A_{\text{inf}} \equiv A(t=t_{\text{inf}})$ and $A_{\text{reh}} \equiv A(t=t_{\text{reh}})$. Here t_{inf} is the physical time at the end of inflation, and t_{reh} is the physical time at the completion of reheating. As the effects of slow-roll parameters are fairly small, the Hubble parameter remains constant throughout the entire epoch of inflation. Thus, H_{inf} could be used to represent the Hubble parameter during inflation.

¹This NCHC scenario differs from the previous cosmological Higgs collider study in the literature [17] in which the inflaton is assumed to couple to certain newly added singlet scalar and predominantly decay into these scalars.

²Adding additional light scalar particle(s) to the Higgs sector at weak scale could lift the Higgs self-coupling to the level of $O(0.1)$ at the inflation scale [20]. For the current study we will just adopt the minimal SM Higgs sector.

2.1 Dynamics of Higgs Field during Inflation

During inflation the universe exponentially expands and can be described by the de Sitter spacetime if the slow-roll of the inflaton is neglected. In contrast to the inflaton, a massless spectator scalar field with self-interaction, will exhibit infrared (IR) divergences in de Sitter spacetime [21–23]. The framework of stochastic inflation [24][25] provides a systematic approach to deal with the IR behavior for the super-horizon mode of the massless spectator field.

Although the SM Higgs doublet \mathbb{H} contains four real scalar components, three of them correspond to the Goldstone modes that become the longitudinal components of the SU(2) weak gauge bosons. During inflation, the fluctuation of Higgs field is on the order of the Hubble parameter, which means the masses of the weak gauge bosons are also of the order of the Hubble scale and thus rather large. On the other hand, the CP even component h of the Higgs doublet \mathbb{H} is much lighter due to the smallness of Higgs self-coupling in comparison with the weak gauge coupling, $\lambda \ll g^2$. Hence for the present study we only need to deal with the light Higgs field h . In the unitary gauge, the Higgs doublet takes the following form:

$$\mathbb{H} = \frac{1}{\sqrt{2}} \begin{pmatrix} 0 \\ h \end{pmatrix}. \quad (2.2)$$

Thus, the Lagrangian density of the pure Higgs sector can be expressed as follows:

$$\mathcal{L} = \sqrt{-g} \left[-\frac{1}{2} g_{\mu\nu} (\partial^\mu h \partial^\nu h) - V(h) \right], \quad (2.3a)$$

$$V(h) = -\frac{1}{2} \mu^2 h^2 + \frac{\lambda}{4} h^4. \quad (2.3b)$$

In the above $V(h)$ is the Higgs potential, in which the quadratic mass term $\frac{1}{2} \mu^2 h^2$ could be omitted for a large value of h during the inflation.

The Higgs field h can be decomposed into a long-wavelength mode (h_L) and the short-wavelength modes (which include contributions above a physical cutoff scale $\epsilon a(t)H$). They are both generated by quantum fluctuations:

$$h(\mathbf{x}, t) = h_L(\mathbf{x}, t) + \int \frac{d^3k}{(2\pi)^3} \theta(k - \epsilon a(t)H_{\text{inf}}) \left[a_{\mathbf{k}} h_{\mathbf{k}}(t) e^{-i\mathbf{k}\cdot\mathbf{x}} + a_{\mathbf{k}}^\dagger h_{\mathbf{k}}^*(t) e^{i\mathbf{k}\cdot\mathbf{x}} \right], \quad (2.4)$$

where ϵ is a small parameter such that the short-wavelength modes satisfy the massless Klein-Gordon equation in the de Sitter space which has the following solution:

$$h_{\mathbf{k}} = \frac{H_{\text{inf}}}{\sqrt{2k^3}} (1 + ik\tau) e^{-ik\tau}, \quad (2.5)$$

where $\tau = -1/(aH)$ is the conformal time.

In this framework, the short-wavelength modes $h_{\mathbf{k}}(t)$ are initially sub-horizon and correspond to the normalized modes of a massless scalar field in the de Sitter spacetime. As the universe expands, these modes are stretched and eventually cross the physical cutoff $\epsilon a(t)H$, transitioning into super-horizon modes h_L . The long-wavelength, super-horizon

modes h_L , can be effectively treated as a classical stochastic field, following the Langevin equation:

$$\dot{h}_L(\mathbf{x}, t) = -\frac{1}{3H_{\text{inf}}} \frac{\partial V}{\partial h_L} + f(\mathbf{x}, t). \quad (2.6)$$

It shows that the evolution of the long-wavelength modes is driven by an effective stochastic “force” $f(\mathbf{x}, t)$, which is generated by the “freezing out” of short-wavelength modes:

$$f(\mathbf{x}, t) = \int \frac{d^3k}{(2\pi)^3} \delta(k - \epsilon a(t) H_{\text{inf}}) \epsilon a(t) H_{\text{inf}}^2 \left(a_{\mathbf{k}} h_{\mathbf{k}} e^{-i\mathbf{k}\cdot\mathbf{x}} + a_{\mathbf{k}}^\dagger h_{\mathbf{k}}^* e^{i\mathbf{k}\cdot\mathbf{x}} \right), \quad (2.7)$$

where we have used the equation $da(t)/dt = H_{\text{inf}} a(t)$, and the two-point correlation function of the stochastic noise $f(\mathbf{x}, t)$ is given by

$$\langle f(\mathbf{x}_1, t_1) f(\mathbf{x}_2, t_2) \rangle = \frac{H_{\text{inf}}^3}{4\pi^2} \delta(t_1 - t_2) j_0(\epsilon a(t_1) H_{\text{inf}} |\mathbf{x}_1 - \mathbf{x}_2|), \quad (2.8)$$

where $j_0(z) = (\sin z)/z$. Hence, the behavior of the Higgs field on super-horizon scales can be described as a classical stochastic process with a probability distribution ρ satisfying a Fokker-Planck (FP) equation:

$$\frac{\partial \rho[h(\mathbf{x}, t)]}{\partial t} = \frac{1}{3H_{\text{inf}}} \frac{\partial}{\partial h} \left\{ \rho[h(\mathbf{x}, t)] \frac{\partial}{\partial h} V[h(\mathbf{x}, t)] \right\} + \frac{H_{\text{inf}}^3}{8\pi^2} \frac{\partial^2}{\partial h^2} \rho[h(\mathbf{x}, t)]. \quad (2.9)$$

The last term on the right-hand side represents the effect of stochastic noise, originating from the sub-horizon modes of the Higgs field as they cross the horizon. This term encapsulates the quantum nature of the fluctuations.

To obtain the probability distribution $\rho(h, t)$, we expand it in terms of a set of eigenfunctions $\Psi_n(h)$ as follows:

$$\rho(h, t) = \Psi_0(h) \sum_{n=0}^{\infty} a_n \Psi_n(h) \exp(-\Lambda_n t), \quad (2.10)$$

where Λ_n and $\Psi_n(h)$ denote the corresponding eigenvalues and eigenfunction of the following differential equation,

$$\tilde{D}_h \Psi_n(h) = -\frac{8\pi^2 \Lambda_n}{H_{\text{inf}}^3} \Psi_n(h). \quad (2.11)$$

In the above, the operator \tilde{D}_h is defined as following:

$$\tilde{D}_h = \frac{\partial^2}{\partial h^2} - \left[\left(\frac{\partial v(h)}{\partial h} \right)^2 - \frac{\partial^2 v(h)}{\partial h^2} \right], \quad (2.12)$$

where $v(h) = [4\pi^2/(3H_{\text{inf}}^4)]V(h)$ and $V(h) = \frac{\lambda}{4}h^4$ is the SM Higgs potential. The eigenfunctions are orthonormalized as follows:

$$\int_{-\infty}^{+\infty} dh \Psi_n(h) \Psi_{n'}(h) = \delta_{n,n'}. \quad (2.13)$$

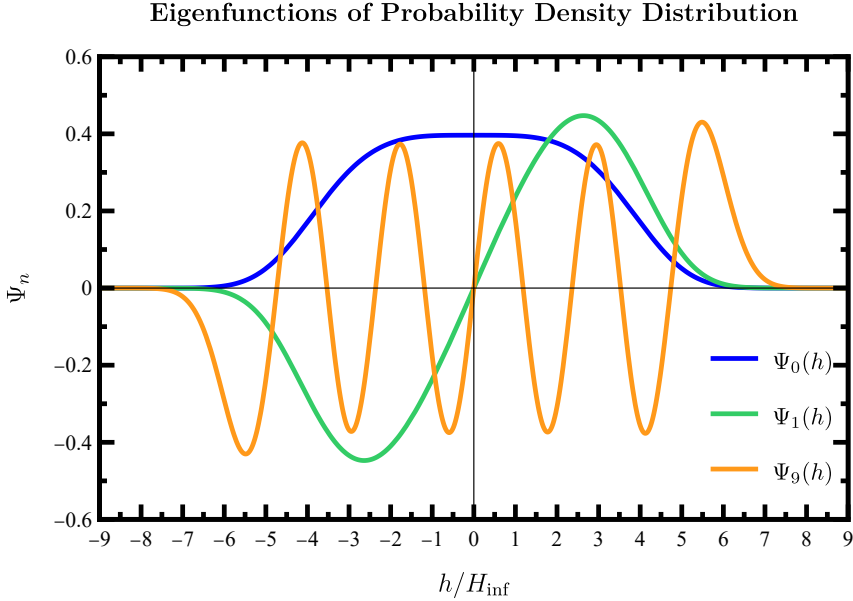


Figure 1. Shape of the eigenfunction Ψ_n as a function of Higgs field h , where we choose the eigenvalue index $n = 0, 1, 9$ for illustration. The SM Higgs self-coupling constant is set as $\lambda = 0.001$.

The derivation of above equations is provided in Appendix D. We note that all the eigenvalues are non-negative and increase with the index n , and the lowest eigenvalue vanishes ($\Lambda_0=0$).

In Fig. 1, we plot the shape of the eigenfunction $\Psi_n(h)$ as a function of the Higgs field h , and we choose the eigenvalue index $n=0, 1, 9$ for illustration. The eigenvalue equation of Eqs.(2.11)-(2.12) is a Sturm-Liouville problem [26] and the eigenfunction $\Psi_n(h)$ is proved to have n zero-points and $n+1$ extremal points.

If inflation lasts for enough time, the only remaining eigenfunction is the ground state eigenfunction $\Psi_0(h)$ corresponding to the eigenvalue $\Lambda_0=0$. Consequently, the probability distribution of the long-wavelength modes asymptotically approaches that of an equilibrium state:

$$\rho_{\text{eq}}(h) = \frac{2\lambda^{1/4}}{\Gamma(1/4)} \left(\frac{2\pi^2}{3}\right)^{1/4} \exp\left(\frac{-2\pi^2\lambda h^4}{3H_{\text{inf}}^4}\right), \quad (2.14)$$

where the normalization is imposed,

$$\int_{-\infty}^{+\infty} dh \rho_{\text{eq}}(h) = 1. \quad (2.15)$$

In Fig. 2, we present the equilibrium probability distribution $\rho_{\text{eq}}(h)$ as a function of the Higgs field h in the unitary gauge.

The root-mean-square value of the Higgs field h can be derived as follows:

$$\bar{h} = \sqrt{\langle h^2 \rangle} = \left[\int_{-\infty}^{+\infty} dh h^2 \rho_{\text{eq}}(h) \right]^{1/2} \simeq 0.363 \left(\frac{H_{\text{inf}}}{\lambda^{1/4}} \right). \quad (2.16)$$

For the present analysis, the SM Higgs self-coupling constant is as $\lambda=0.001$, corresponding to $\bar{h} \simeq 2H_{\text{inf}}$. The scale of the observable universe with $N_e \sim 60$ leads to $\lambda N_e < 1$, indicating

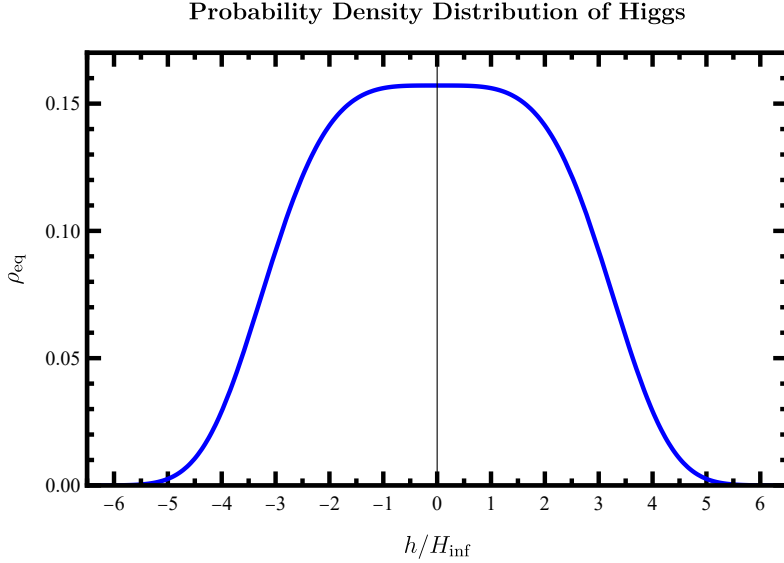


Figure 2. Probability density distribution ρ_{eq} as a function of the Higgs field h at the end of inflation. The SM Higgs self-coupling constant is set as $\lambda=0.001$.

that the loop effects are generally small in our observable universe [22][23]. Thus the Higgs field in our universe can be approximated by a uniform background $\bar{h} \simeq H_{\text{inf}}/\lambda^{1/4}$ combined with quantum fluctuations $\delta h(\mathbf{x}, t)$ around the mean value \bar{h} , namely,

$$h(\mathbf{x}, t) = \bar{h}(t) + \delta h(\mathbf{x}, t), \quad (2.17)$$

which enables the application of the mean field (MF) approximation in the subsequent analysis. In order to obtain the mode functions of the quantum fluctuation $\delta h(\mathbf{x}, t)$, we expand Eq.(2.1) by substituting $h(\mathbf{x}, t) = \bar{h}(t) + \delta h(\mathbf{x}, t)$ to obtain the Lagrangian for δh

$$\mathcal{L}(\delta h) \rightarrow \sqrt{-g} \left[-\frac{1}{2} \partial_\mu \delta h \partial^\mu \delta h + \frac{1}{2} \mu^2 (\delta h)^2 - \frac{3}{2} \lambda \bar{h}^2 (\delta h)^2 - (\lambda \bar{h}) \delta h^3 - \frac{\lambda}{4} \delta h^4 \right]. \quad (2.18)$$

In the MF approximation, the field δh is taken to be the linear solution to the equation of motion. The mass of the Higgs fluctuation is $m_{\delta h}^2 = 3\lambda \bar{h}^2 - \mu^2 \simeq 0.4\lambda^{1/2} H_{\text{inf}}^2$, which means the mass of the fluctuation δh is suppressed by the SM Higgs self-coupling constant λ . In this case, the mass of the Higgs fluctuation is $m_{\delta h}$ could easily satisfy $m_{\delta h}^2 \ll H_{\text{inf}}^2$ with a small λ .

For convenience, we use the approximation that the fluctuation δh is massless and thus the mode functions of $\delta h(\mathbf{k})$ are also the solution for the massless Klein-Gordon equation in the de Sitter spacetime, as shown in Eq.(2.5).

2.2 Evolution of Higgs Field after Inflation

After inflation, if the inflaton potential is quadratic around the bottom of the potential, the inflaton would oscillate and behave like the cold matter ($w=0$) having a mass $m_\phi \sim O(1-10)H_{\text{inf}}$. Consequently, the universe will expand as $a(t) \sim t^{2/3}$, from which the Hubble parameter is given by $H = 2/(3t)$. Using the Lagrangian (2.1) and considering only the

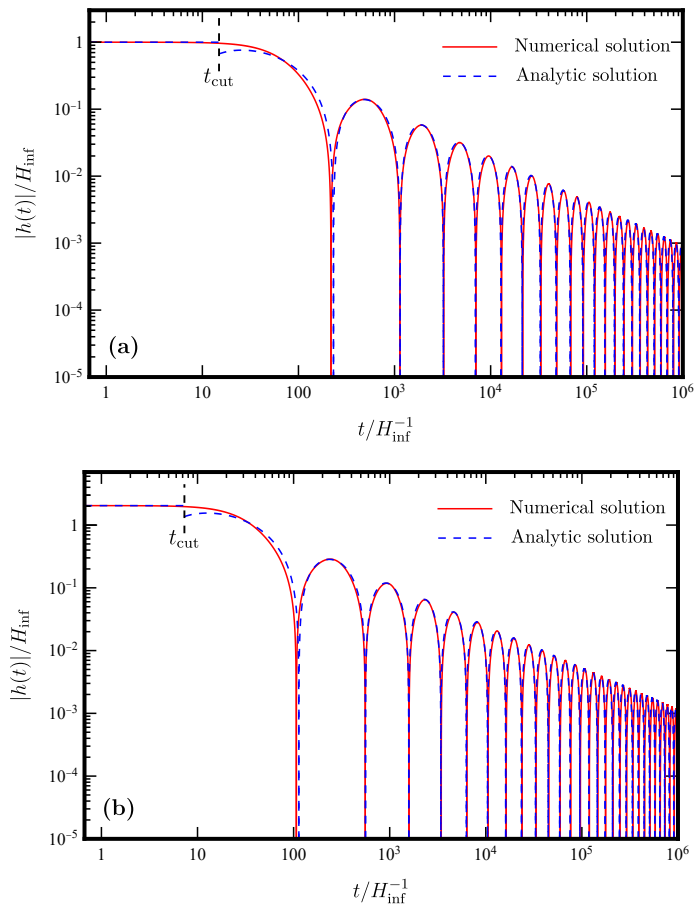


Figure 3. Evolution of background value of the Higgs field $|h(t)|$ after inflation, where we set the initial value $h_{\text{inf}} = H_{\text{inf}}$ in plot (a) and $h_{\text{inf}} = \bar{h} \simeq 2H_{\text{inf}}$ [according to Eq.(2.16)] in plot (b). In each plot, the red solid curve represents the numerical solution and the blue dashed curve denotes the analytic solution.

quartic term of the Higgs potential, we find that the evolution of the super-horizon mode of the Higgs field after inflation is described by the following Klein-Gordon equation:

$$\ddot{h}(t) + \frac{2}{t}\dot{h}(t) + \lambda h^3(t) = 0. \quad (2.19)$$

We solve Eq.(2.19) numerically to determine the evolution of the Higgs field h . The results are presented in Fig. 3, where the Higgs self-coupling constant is set as $\lambda = 0.001$. We further set the initial value $h_{\text{inf}} = H_{\text{inf}}$ in plot (a) and $h_{\text{inf}} = \bar{h} \simeq 2H_{\text{inf}}$ [according to Eq.(2.16)] in plot (b). In each plot, the red solid curve represents the numerical solution, whereas the blue dashed curve denotes the analytic solution.

Besides, we present a semi-analytical solution to Eq.(2.19) which is given in Appendix A. In the following, we derive the analytical formulas for the evolution of the Higgs

field $h(t)$ in the case of $h_{\text{inf}} > 0$:

$$h(t) = \begin{cases} h_{\text{inf}}, & t \leq t_{\text{cut}}, \\ AH_{\text{inf}} \left(\frac{h_{\text{inf}}}{H_{\text{inf}} \lambda} \right)^{\frac{1}{3}} (H_{\text{inf}} t)^{-\frac{2}{3}} \cos \left(\lambda^{\frac{1}{6}} h_{\text{inf}}^{\frac{1}{3}} \omega t^{\frac{1}{3}} + \theta \right), & t > t_{\text{cut}}, \end{cases} \quad (2.20)$$

where the relevant parameters are given as follows,

$$t_{\text{cut}} = \frac{\sqrt{2}}{3\sqrt{\lambda} h_{\text{inf}}}, \quad A = \left(\frac{2}{9} \right)^{\frac{1}{3}} 5^{\frac{1}{4}} \simeq 0.9, \quad (2.21a)$$

$$\omega = \frac{\Gamma^2(3/4)}{\sqrt{\pi}} \left(\frac{2}{3} \right)^{\frac{1}{3}} 5^{\frac{1}{4}} \simeq 2.3, \quad \theta = -3^{-\frac{1}{3}} 2^{\frac{1}{6}} \omega - \arctan 2 \simeq -2.9. \quad (2.21b)$$

One can readily derive the solution for the case $h_{\text{inf}} < 0$. In Fig. 3, we compare the numerical solutions with our analytic solution. We find that for $t \gg t_{\text{cut}}$ the analytic solution agrees with the numerical results very well. This result indicates that after inflation the Higgs field would oscillate in its quartic potential $\frac{1}{4}\lambda h^4$ and the amplitude of these oscillations will decay due to Hubble friction.

3 Higgs Modulated Reheating Using Right-handed Neutrino

In this section, we present a minimal realization incorporating inflation and neutrino seesaw, in which the inflaton decay is modulated by the Higgs boson through right-handed neutrino. We will give the model realization and setup in Section 3.1 and study the Higgs modulated reheating through right-handed neutrino in Section 3.2.

3.1 Model Realization and Setup

In addition to the particle content of the Standard Model (SM), we introduce the scalar field inflaton ϕ and right-handed neutrinos N_R . The relevant Lagrangian is given as follows:

$$\Delta\mathcal{L} = \sqrt{-g} \left[-\frac{1}{2} \partial_\mu \phi \partial^\mu \phi - V(\phi) + \bar{N}_R i \not{\partial} N_R + \frac{1}{\Lambda} \partial_\mu \phi \bar{N}_R \gamma^\mu \gamma^5 N_R + \left(-\frac{1}{2} M \bar{N}_R^c N_R - y_\nu \bar{\ell}_L \tilde{\mathbb{H}} N_R + \text{H.c.} \right) \right], \quad (3.1)$$

where \mathbb{H} is the SM Higgs doublet and $\tilde{\mathbb{H}} = i\sigma_2 \mathbb{H}^*$ with σ_2 the second Pauli matrix. In Eq.(3.1) $V(\phi)$ is the inflaton potential and its concrete form is irrelevant to the following discussion. After inflation the potential $V(\phi)$ is assumed to be dominated by the inflaton mass term under which the inflaton ϕ will oscillate. In the above we have suppressed the flavor indices for the SM leptons and right-handed neutrinos. Each lepton doublet $\ell_L = (\nu_L, e_L)^T$ interacts with a right-handed neutrino N_R through the Yukawa coupling y_ν , which is generally a complex matrix. Due to the shift symmetry, the inflaton ϕ couples to the right-handed neutrinos through a dimension-5 effective operator with cutoff Λ . To maintain the perturbative unitarity of the theory during inflation requires Λ to be no less than $60H_{\text{inf}}$, namely, $\Lambda \geq (\dot{\phi})^{1/2} \simeq 60H_{\text{inf}}$. The shift symmetry plays a key role

for maintaining the flatness of the inflaton potential throughout inflation, and is widely realized in models such as the natural inflation [27] and axion monodromy inflation [28][29], or other models with inflation driven by pseudo-Nambu-Goldstone bosons. The inflaton may couple to SM fermions or gauge bosons through higher-dimensional operators, allowing it to decay into SM particles which are usually suppressed. Consequently, the inflaton is expected to primarily decay into right-handed neutrinos.

For simplicity, we will focus on the case of one generation of fermions for the present study. In this case, the neutrino mass matrix is shown as follows:

$$\mathbf{M}_\nu = \begin{pmatrix} 0 & \frac{y_\nu h}{\sqrt{2}} \\ \frac{y_\nu h}{\sqrt{2}} & M \end{pmatrix}. \quad (3.2)$$

By diagonalizing the neutrino seesaw mass matrix, we derive the neutrino mass-eigenstates of ν and N as follows:³

$$m_\nu \simeq -\frac{y_\nu^2 h^2}{2M}, \quad M_N \simeq M + \frac{y_\nu^2 h^2}{2M}, \quad (3.3)$$

for $M \gg |y_\nu h|$. The mixing angle θ for diagonalizing \mathbf{M}_ν is given by

$$\tan \theta = \frac{\sqrt{2}y_\nu h}{\sqrt{M^2 + 2y_\nu^2 h^2} + M} \simeq \frac{y_\nu h}{\sqrt{2}M}. \quad (3.4)$$

In the above, we see that the heavy neutrino mass-eigenvalue is shifted by an amount of $\frac{y_\nu^2 h^2}{2M}$ relative to M . This lifting effect is crucial for our mechanism to work, as we are actually probing the seesaw scale of the heavy neutrino mass eigenvalue.

In the Lagrangian (3.1), the inflaton is coupled to the right-handed neutrino N_R through a dimension-5 operator $\frac{1}{\Lambda} \partial_\mu \phi \bar{N}_R \gamma^\mu \gamma^5 N_R$. After inflation, the inflaton decays through this operator until the reheating completes. The inflaton should decay into the mass eigenstates (ν and N) instead of chiral eigenstates (ν_L and N_R). So in terms of mass eigenstates the relevant interaction vertices from this dimension-5 operator take the following form:

$$\frac{\cos^2 \theta}{\Lambda} \partial_\mu \phi \bar{N} \gamma^\mu \gamma^5 N + \frac{\sin^2 \theta}{\Lambda} \partial_\mu \phi \bar{\nu} \gamma^\mu \gamma^5 \nu - \left(\frac{\sin 2\theta}{2\Lambda} \partial_\mu \phi \bar{N} \gamma^\mu \gamma^5 \nu + \text{h.c.} \right). \quad (3.5)$$

Hence, there are three decay channels $\phi \rightarrow NN, N\nu, \nu\nu$. Thus, we compute the decay rates of the inflaton as follows:

$$\Gamma(\phi \rightarrow NN) = \frac{m_\phi M_N^2 \cos^4 \theta}{4\pi \Lambda^2} \left(1 - \frac{4M_N^2}{m_\phi^2} \right)^{1/2}, \quad (3.6a)$$

$$\Gamma(\phi \rightarrow N\nu) = \frac{m_\phi M_N^2 (\sin 2\theta)^2}{32\pi \Lambda^2} \left(1 - \frac{M_N^2}{m_\phi^2} \right)^2, \quad (3.6b)$$

³For the parameter space, we consider that the value of $y_\nu h/M$ always satisfies the condition $|y_\nu h/M| \ll 1$ at the time of reheating.

$$\Gamma(\phi \rightarrow \nu\nu) = \frac{m_\phi m_\nu^2 \sin^4 \theta}{4\pi\Lambda^2} \left(1 - \frac{4m_\nu^2}{m_\phi^2}\right)^{1/2}, \quad (3.6c)$$

where the last decay rate $\Gamma(\phi \rightarrow \nu\nu)$ is suppressed by light neutrino mass factor m_ν^2 and is thus fully negligible. Since the mixing angle $\theta \simeq \frac{y_\nu h}{\sqrt{2}M} \ll 1$, we see that the inflaton decay is dominated by the channel $\phi \rightarrow NN$. Consequently, if we neglect the kinematic factors in the above formula, the total decay rate of the inflaton can be approximated as follows:

$$\Gamma \simeq \frac{m_\phi M^2}{4\pi\Lambda^2} \left[1 + \frac{1}{4} \left(\frac{y_\nu h}{M}\right)^2\right]. \quad (3.7)$$

In our setup, the reheating occurs instantaneously at the time $\Gamma = H(t_{\text{reh}}) = 2/(3t_{\text{reh}})$. Eq. 3.7 shows that the decay of the inflaton through the right-handed neutrino is modulated by the Higgs, and then the Higgs fluctuation would induce the curvature perturbation.

Note that our scenario differs from the inflaton decays through the SM fermion channel, where $\Gamma \propto m_f^2 \propto (y_f h)^2$. Since the Higgs field value decreases after inflation, the decay width of inflaton $\Gamma \propto h^2$ would decrease even faster than the Hubble parameter $H(t)$, preventing the completion of reheating [17]. But, unlike the SM fermions, the mass of the right-handed neutrino is mainly contributed by the Majorana mass M instead of the Higgs field value h . This feature prevents the inflaton decay rate Γ from fast decreasing with h . Thus, a viable Higgs-modulated reheating can be realized. We note that the conventional seesaw mechanism has the seesaw scale M typically around 10^{14} GeV, which is comparable to the Hubble scale H_{inf} during inflation. We consider the parameter space of $M_N < m_\phi/2$, and thus the inflaton decaying into two heavy neutrinos is generally kinetically allowed. There are also other dimension-5 operators such as $\frac{1}{\Lambda} \partial_\mu \phi \bar{f} \gamma^\mu \gamma^5 f$ with f being the SM fermions, but these operators do not affect our final result. This is because the inflaton should predominantly decay into the heavy neutrinos and its decays into the SM fermions are much suppressed as the SM fermion masses are proportional to h which already becomes much smaller during reheating.

In passing, we note that our model differs from the literature [30], where a right-handed neutrino is introduced and its mass is modulated solely due to the Dirac mass term and the curvature perturbation is from the kinematic blocking of inflaton decays. In our model, the modulation arises from the neutrino seesaw mechanism. Besides, the model of [30] has inflaton couple to the right-handed neutrino via a dimension-4 operator without shift symmetry, which would induce a large Planck-scale Majorana mass term for the right-handed neutrino and could make the inflaton decay difficult. In our model, the inflaton has derivative coupling with the right-handed neutrinos under the shift symmetry, so it does not directly contribute to the Majorana mass of the right-handed neutrinos.

We note that the derivative coupling between inflaton and heavy neutrino can also induce cosmological collider signals during the inflation [31][32]. For the present study, our primary focus is on the predictions for the local type f_{NL} which is generated from the Higgs modulated reheating through neutrino seesaw. This differs from the conventional cosmological collider signals generated by the inflaton correlation functions during inflation (which does not invoke Higgs modulated reheating).

3.2 Higgs Modulated Reheating

In our model, the decay rate of inflaton is influenced by the SM Higgs field. Fluctuations of the Higgs field value (as generated during inflation) cause variations in the inflaton's decay rate across different Hubble patches. These variations perturb the local expansion history, seeding large-scale inhomogeneity and anisotropy in the universe through these Higgs fluctuations. The δN formalism [33–41] can be used to compute these fluctuations. The number of e-folds of the cosmic expansion after inflation can be derived as follows:

$$\begin{aligned}
 N(\mathbf{x}) &= \int d \ln a(t) = \int_{t_{\text{inf}}}^{t_{\text{reh}}(\mathbf{x})} dt H(t) + \int_{t_{\text{reh}}(\mathbf{x})}^{t_f} dt H(t) \\
 &= \int_{\rho_{\text{inf}}}^{\rho_{\text{reh}}(h(\mathbf{x}))} d\rho \frac{H}{\dot{\rho}} + \int_{\rho_{\text{reh}}(h(\mathbf{x}))}^{\rho_f} d\rho \frac{H}{\dot{\rho}}, \tag{3.8}
 \end{aligned}$$

where $a(t)$ is the scale factor, $\rho(t)$ is the total energy density of the universe at the time t , t_{inf} is the physical time at the end of inflation, t_{reh} is the physical time at which reheating occurs, ρ_f is a reference energy density and t_f is the reference time where the energy density $\rho = \rho_f$ after the completion of reheating.

For the present study, we consider the universe as a perfect fluid, both before and after the completion of reheating. At the end of inflation (t_{inf}), we assume the inflaton's decay rate Γ is significantly smaller than the Hubble scale. Reheating is completed at a subsequent time t_{reh} when the Hubble parameter satisfies $H(t_{\text{reh}}) = \Gamma_{\text{reh}}$. As discussed in the previous section, during the period before reheating completion ($t_{\text{inf}} < t < t_{\text{reh}}$), the inflaton oscillates near the minimum of a quadratic potential. This corresponds to the matter-dominated universe, where the pressure $p = 0$ and thus the equation of state parameter $w = p/\rho = 0$. Throughout this stage, the universe expands as $a \sim t^{2/3}$, with the Hubble parameter $H = 2/(3t)$. After reheating completes ($t > t_{\text{reh}}$), the universe becomes radiation-dominated, which means that the equation of state parameter is $w = 1/3$ and the scale factor behaves as $a \sim t^{1/2}$, with the Hubble parameter given by $H = 1/(2t)$. Here the right-handed neutrinos decay fast enough after being produced.

As a result, the state of the universe changes before and after the completion of reheating. For a fluctuation $\delta\Gamma_{\text{reh}}(\mathbf{x})$ in the decay rate, there will be variations in the local reheating time $t_{\text{reh}}(\mathbf{x})$ across different Hubble patches. These variations translate into differences in the expansion history among these patches, which can be quantitatively expressed as fluctuations in the number of e-folds $\delta N(\mathbf{x}, t)$ of local expansion after inflation.

On the other hand, the comoving curvature perturbation after reheating, $\zeta_h(\mathbf{x}, t)$, is equal to the $\delta N(\mathbf{x}, t)$ of cosmic expansion among different Hubble patches under the uniform energy density gauge,

$$\zeta_h(\mathbf{x}, t) = \delta N(\mathbf{x}, t) = N(\mathbf{x}, t) - \langle N(\mathbf{x}, t) \rangle. \tag{3.9}$$

Since the Higgs fluctuation causes the fluctuation of the inflaton decay rate $\delta\Gamma_{\text{reh}}(\mathbf{x})$ in the Higgs-modulated reheating, we can express the comoving curvature perturbation as

a function of the local Higgs fluctuation $h(\mathbf{x}, t_{\text{reh}})$. By utilizing the continuity equation

$$\dot{\rho} + 3H(1+w)\rho = 0, \quad (3.10)$$

we integrate Eq.(3.8) and derive the local e-folding number:

$$N(\mathbf{x}) = -\frac{1}{3(1+w_1)} \ln \frac{\rho_{\text{reh}}(h(\mathbf{x}))}{\rho_{\text{inf}}} - \frac{1}{3(1+w_2)} \ln \frac{\rho_f}{\rho_{\text{reh}}(h(\mathbf{x}))}, \quad (3.11)$$

where $w_1 = 0$ is the equation of state parameter before reheating is completed,⁴ and the equation of state parameter after reheating is $w_2 = 1/3$. Utilizing the first Friedmann equation $3H^2 M_p^2 = \rho$ and noting that reheating completes when $H(t_{\text{reh}}) = \Gamma_{\text{reh}}$ is reached, we can derive the following comoving curvature perturbation after reheating ($t > t_{\text{reh}}$):

$$\begin{aligned} \zeta_h(\mathbf{x}, t > t_{\text{reh}}) &= \delta N(\mathbf{x}) = N(\mathbf{x}) - \langle N(\mathbf{x}) \rangle \\ &= -\frac{1}{12} [\ln \rho_{\text{reh}}(\mathbf{x}) - \langle \ln \rho_{\text{reh}}(\mathbf{x}) \rangle] \\ &= -\frac{1}{6} [\ln(H_{\text{reh}}) - \langle \ln(H_{\text{reh}}) \rangle] \\ &= -\frac{1}{6} [\ln(\Gamma_{\text{reh}}) - \langle \ln(\Gamma_{\text{reh}}) \rangle]. \end{aligned} \quad (3.12)$$

In this scenario, we derive a relationship between curvature perturbation $\zeta_h(\mathbf{x})$ from Higgs-modulated reheating and the Higgs field h_{inf} during inflation, as illustrated in Fig. 4.

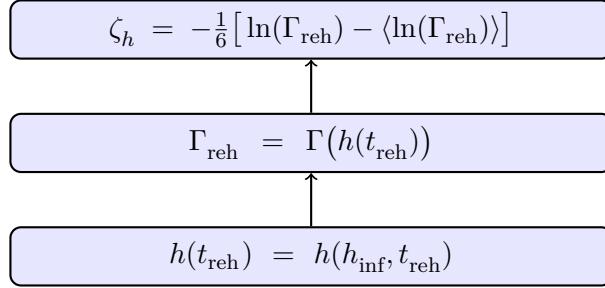


Figure 4. Schematic plot showing how the comoving curvature perturbation ζ_h sourced from the Higgs modulated reheating is a function of the Higgs field h_{inf} during the inflation, $\zeta_h = \zeta_h(h_{\text{inf}})$.

In Section 2, we have demonstrated that the value of the Higgs field at the completion of reheating, $h(t_{\text{reh}})$, is determined by the initial value of h_{inf} . Given that the inflaton's decay rate Γ is a function of the Higgs value $h(t_{\text{reh}})$ from Eq.(3.3) and Eq.(3.6), and that the comoving curvature perturbation ζ depends on the decay rate Γ , we can thus establish a relationship between the comoving curvature perturbation ζ and the Higgs field h_{inf} during inflation.

Note that at the time of the reheating occurring, the value of the Higgs field after inflation becomes an oscillatory function of its initial value,

$$h(t_{\text{reh}}, h_{\text{inf}}) \sim (h_{\text{inf}})^{\frac{1}{3}} \cos\left(\omega_{\text{reh}} h_{\text{inf}}^{\frac{1}{3}} + \theta\right), \quad (3.13)$$

⁴Our approach also applies to the general case of $w_1 \neq 1/3$.

with the oscillating frequency estimated as

$$\omega_{\text{reh}} = \lambda^{\frac{1}{6}} t_{\text{reh}}^{\frac{1}{3}} \omega. \quad (3.14)$$

When t_{reh} is large, the oscillation frequency can become very high. Note that ζ_h is a function of h^2 and can be expanded into the form $A+Bh^2/M^2+O(h^4/M^4)$, which includes a factor $\cos^2(\omega_{\text{reh}} h_{\text{inf}}^{1/3} + \theta)$. Since h_{inf} varies across different Hubble volumes and ζ_h is highly sensitive to h_{inf} , averaging over a sufficiently large volume allows the factor $\cos^2(\omega_{\text{reh}} h_{\text{inf}}^{1/3} + \theta)$ to be effectively treated as $1/2$ [42]. Consequently, in the subsequent calculations, we directly set $\cos^2(\omega_{\text{reh}} h_{\text{inf}}^{1/3} + \theta) \rightarrow 1/2$.

Combined with the inflaton fluctuation $\delta\phi$ during inflation, the total comoving curvature perturbation can be written as follows:

$$\zeta = \zeta_\phi + \zeta_h, \quad (3.15)$$

where ζ_ϕ is generated by the inflaton fluctuation $\delta\phi$,

$$\zeta_\phi \simeq -\frac{H_{\text{inf}}}{\dot{\phi}_0} \delta\phi(\mathbf{x}), \quad (3.16)$$

and ζ_h originates from the Higgs-modulated reheating. Because these two components are generated at different times and are independent of each other, the power spectrum of ζ contains both contributions:

$$\mathcal{P}_\zeta = \mathcal{P}_\zeta^{(\phi)} + \mathcal{P}_\zeta^{(h)}, \quad (3.17)$$

where $\mathcal{P}_\zeta^{(\phi)}$ denotes the contribution induced by inflaton fluctuations,

$$\mathcal{P}_\zeta^{(\phi)} = \left(\frac{H}{\dot{\phi}}\right)^2 \mathcal{P}_\phi = \left(\frac{H_{\text{inf}}}{\dot{\phi}_0}\right)^2 \frac{H_{\text{inf}}^2}{4\pi^2}. \quad (3.18)$$

For convenience, we define R as square root of the ratio between the power spectrum of the Higgs-modulated reheating and that of the comoving curvature perturbation ζ ,

$$R \equiv \left(\frac{\mathcal{P}_\zeta^{(h)}}{\mathcal{P}_\zeta}\right)^{1/2}. \quad (3.19)$$

In the literature various modulated reheating models were studied, which often assume that all primordial perturbations originate from Higgs-modulated reheating ($R=1$) [30][43–46]. The existing cosmological observations require $R < 1$. In this work, we compute $\mathcal{P}_\zeta^{(h)}$ through the mean field method and impose $R < 1$ for our parameter space.

Moreover, the modulated reheating can provide a source of primordial non-Gaussianity (NG). Primordial non-Gaussianity is characterized by the three-point correlation function of ζ , which is also called the bispectrum $\langle \zeta_{\mathbf{k}_1} \zeta_{\mathbf{k}_2} \zeta_{\mathbf{k}_3} \rangle$. This primordial non-Gaussianity leaves an imprint on the CMB anisotropy and large-scale structure observations. Different physics effects involved during inflation lead to different shape functions of the primordial NG, and several templates of shape functions are measured by using the Planck-2018 data

to identify signals of potential new physics [3–5]. For instance, the local non-Gaussianity of the Bardeen potential Φ is given by

$$\langle \Phi_{\mathbf{k}_1} \Phi_{\mathbf{k}_2} \Phi_{\mathbf{k}_3} \rangle'_{\text{local}} = 2A^2 f_{\text{NL}}^{\text{local}} \left\{ \frac{1}{k_1^3 k_2^3} + \frac{1}{k_2^3 k_3^3} + \frac{1}{k_3^3 k_1^3} \right\}. \quad (3.20)$$

In the above, $\langle \Phi_{\mathbf{k}_1} \Phi_{\mathbf{k}_2} \Phi_{\mathbf{k}_3} \rangle'$ is defined as the 3-point correlation function excluding the delta function of momentum conservation, $\langle \Phi_{\mathbf{k}_1} \Phi_{\mathbf{k}_2} \Phi_{\mathbf{k}_3} \rangle = (2\pi)^3 \delta^3(\mathbf{k}_1 + \mathbf{k}_2 + \mathbf{k}_3) \langle \Phi_{\mathbf{k}_1} \Phi_{\mathbf{k}_2} \Phi_{\mathbf{k}_3} \rangle'$.

For studying the modulated reheating, the comoving curvature perturbation ζ is expanded as a function of the fluctuation of the Higgs field during the inflation δh_{inf} around its mean value \bar{h} :

$$\zeta_h(\delta h_{\text{inf}}(\mathbf{x})) = \delta N(\delta h_{\text{inf}}(\mathbf{x})) = N' \delta h_{\text{inf}} + \frac{1}{2} N'' (\delta h_{\text{inf}})^2 + \dots, \quad (3.21)$$

where N' and N'' denote the first and second derivatives of the e-folding number N with respect to the Higgs field δh_{inf} , evaluated at its mean value:

$$N' = \left. \frac{dN}{dh_{\text{inf}}} \right|_{\bar{h}}, \quad N'' = \left. \frac{d^2 N}{dh_{\text{inf}}^2} \right|_{\bar{h}}. \quad (3.22)$$

This perturbative approach is also referred to as the mean-field method and has been commonly used to calculate the n -point correlation functions of curvature perturbation. Using this expansion, we can determine the amplitude of curvature perturbations $\mathcal{P}_\zeta = N'^2 \mathcal{P}_{\delta h}$ and the primordial local non-Gaussianity [43–47].

4 Probing Neutrino Seesaw Using Primordial Non-Gaussianity

As discussed in Section 3.2, for the scenario of Higgs modulated reheating, the fluctuation of the Higgs field can contribute to the comoving curvature perturbation ζ with a fraction R . Moreover, the Higgs-modulated reheating will also generate primordial non-Gaussianities (NG), which could be detected by the CMB or large scale structure observations. In this section, we investigate the primordial local non-Gaussianity arising from the Higgs-modulated reheating. We will demonstrate that the primordial non-Gaussianity provides a viable approach to probe the neutrino seesaw scale. For this purpose, we compute the 2-point and 3-point correlation functions of the comoving curvature perturbation from the Higgs modulated reheating ζ_h . In this section, the Hubble scale during inflation H_{inf} is abbreviated as H , and the notation of Higgs field value during inflation h_{inf} is simplified as h which differs from the Higgs field value $h(t)$ after inflation.

4.1 Analysis of Comoving Curvature Perturbation

As discussed in the Section 3.2, the comoving curvature perturbation ζ from the Higgs modulated reheating depends on the logarithm of decay rate at the completion of reheating $\ln(\Gamma_{\text{reh}})$, as described by Eq.(3.12).

The relation between Γ_{reh} and the Higgs field h_{inf} during inflation is shown in the Fig. 4, namely, $\Gamma_{\text{reh}} = \Gamma(h_{\text{reh}}(t_{\text{reh}}, h_{\text{inf}}))$. In the mean field approximation, we expand the

comoving curvature perturbation to the order of δh_{inf}^2 :

$$\zeta_h(\mathbf{x}) = -\frac{1-3w}{6(1+w)} \left[\frac{\Gamma'_0}{\Gamma_0} \delta h_{\text{inf}}(\mathbf{x}) + \frac{\Gamma_0 \Gamma''_0 - \Gamma'_0 \Gamma'_0}{2\Gamma_0^2} \delta h_{\text{inf}}^2(\mathbf{x}) \right], \quad (4.1)$$

where we have defined,

$$\Gamma_0 = \Gamma_{\text{reh}}|_{h_{\text{inf}}(\mathbf{x})=\bar{h}}, \quad (4.2a)$$

$$\Gamma'_0 = \frac{d\Gamma_{\text{reh}}}{dh_{\text{inf}}} \Big|_{h_{\text{inf}}(\mathbf{x})=\bar{h}} = \frac{d\Gamma_{\text{reh}}}{dh_{\text{reh}}} \frac{\partial h_{\text{reh}}}{\partial h_{\text{inf}}} \Big|_{h_{\text{inf}}(\mathbf{x})=\bar{h}}, \quad (4.2b)$$

$$\Gamma''_0 = \frac{d^2\Gamma_{\text{reh}}}{dh_{\text{inf}}^2} \Big|_{h_{\text{inf}}(\mathbf{x})=\bar{h}} = \frac{d^2\Gamma_{\text{reh}}}{dh_{\text{reh}}^2} \left(\frac{\partial h_{\text{reh}}}{\partial h_{\text{inf}}} \right)^2 \Big|_{h_{\text{inf}}(\mathbf{x})=\bar{h}} + \frac{d\Gamma_{\text{reh}}}{dh_{\text{reh}}} \left(\frac{\partial^2 h_{\text{reh}}}{\partial h_{\text{inf}}^2} \right) \Big|_{h_{\text{inf}}(\mathbf{x})=\bar{h}}. \quad (4.2c)$$

After inflation the inflaton potential is quadratic, so the universe is matter-dominated, implying $w = 0$. We can establish the relation between the curvature perturbation and the Higgs fluctuation as follows:

$$\zeta_h(\mathbf{x}) = -\frac{1}{6} \left[\frac{\Gamma'_0}{\Gamma_0} \delta h_{\text{inf}}(\mathbf{x}) + \frac{\Gamma_0 \Gamma''_0 - \Gamma'_0 \Gamma'_0}{2\Gamma_0^2} \delta h_{\text{inf}}^2(\mathbf{x}) \right] \equiv z_1 \delta h_{\text{inf}}(\mathbf{x}) + \frac{1}{2} z_2 \delta h_{\text{inf}}^2(\mathbf{x}), \quad (4.3)$$

where z_1 and z_2 are the linear and second order coefficients:

$$z_1 = -\frac{1}{6} \frac{\Gamma'_0}{\Gamma_0}, \quad z_2 = -\frac{1}{6} \left[\frac{\Gamma_0 \Gamma''_0 - \Gamma'_0 \Gamma'_0}{\Gamma_0^2} \right]. \quad (4.4)$$

In the following, since we only deal with Higgs fluctuations δh_{inf} during the inflation, we will omit the subscript ‘‘inf’’ and directly use the notation δh for convenience, i.e. $\delta h \equiv \delta h_{\text{inf}}$.

From Eq.(4.3), we further derive the corresponding form in Fourier space:

$$\begin{aligned} \zeta_h(\mathbf{k}) &= \int d^3 \mathbf{x} \zeta(\mathbf{x}) e^{-i\mathbf{k}\cdot\mathbf{x}} = z_1 \delta h(\mathbf{k}) + \frac{z_2}{2} \int d^3 \mathbf{x} \delta h^2(\mathbf{x}) e^{-i\mathbf{k}\cdot\mathbf{x}} \\ &= z_1 \delta h(\mathbf{k}) + \frac{z_2}{2} \int d^3 \mathbf{x} \frac{d^3 \mathbf{k}_1}{(2\pi)^3} \frac{d^3 \mathbf{k}_2}{(2\pi)^3} \delta h(\mathbf{k}_1) \delta h(\mathbf{k}_2) e^{i(\mathbf{k}_1+\mathbf{k}_2-\mathbf{k})\cdot\mathbf{x}} \\ &= z_1 \delta h(\mathbf{k}) + \frac{z_2}{2} \int \frac{d^3 \mathbf{k}_1}{(2\pi)^3} \delta h(\mathbf{k}_1) \delta h(\mathbf{k}-\mathbf{k}_1). \end{aligned} \quad (4.5)$$

Thus, we derive the 2-point correlation function of ζ from the Higgs modulated reheating to the leading order:

$$\langle \zeta_{\mathbf{k}_1} \zeta_{\mathbf{k}_2} \rangle_h = z_1^2 \langle \delta h_{\mathbf{k}_1} \delta h_{\mathbf{k}_2} \rangle, \quad (4.6)$$

from which we obtain the power spectrum of ζ :

$$\mathcal{P}_\zeta^{(h)} = z_1^2 \mathcal{P}_{\delta h} = \frac{z_1^2 H^2}{4\pi^2}. \quad (4.7)$$

In this case, the contribution from Higgs-modulated reheating to the comoving curvature perturbation ζ is given by

$$R = \left(\frac{\mathcal{P}_\zeta^{(h)}}{\mathcal{P}_\zeta} \right)^{1/2} = |z_1| \left(\frac{\mathcal{P}_{\delta h}}{\mathcal{P}_\zeta} \right)^{1/2}. \quad (4.8)$$

We require that the contribution of curvature perturbation from the Higgs-modulated reheating is less than unity, i.e., $R = (\mathcal{P}_\zeta^{(h)}/\mathcal{P}_\zeta)^{1/2} < 1$.

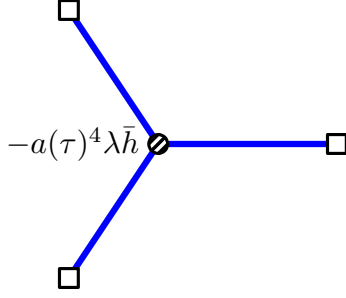


Figure 5. Three-point correlation function of δh from the Higgs self-interaction $\Delta\mathcal{L} = -(\lambda\bar{h})\delta h^3$. The Higgs propagator is depicted by a blue solid line with a dot and a square at its endpoints, representing a bulk-to-boundary propagator, which includes one “plus-type” and one “minus-type”. The square at one end of the propagator indicates its boundary point ($\tau_f \rightarrow 0^-$). The shaded dot at the vertex means that contributions from both plus- and minus-type propagators must be summed.

4.2 Three-Point Correlation Function of Curvature Perturbation

In this subsection, we derive the three-point correlation function of the comoving curvature perturbation ζ contributed by the Higgs modulated reheating, $\zeta_h = z_1\delta h + \frac{1}{2}z_2\delta h^2$. The three-point correlation function of ζ from modulated reheating $\langle\zeta_{\mathbf{k}_1}\zeta_{\mathbf{k}_2}\zeta_{\mathbf{k}_3}\rangle_h$ consists of two parts:

$$\langle\zeta_{\mathbf{k}_1}\zeta_{\mathbf{k}_2}\zeta_{\mathbf{k}_3}\rangle_h = z_1^3\langle\delta h_{\mathbf{k}_1}\delta h_{\mathbf{k}_2}\delta h_{\mathbf{k}_3}\rangle + z_1^2z_2\langle\delta h^4\rangle(\mathbf{k}_1, \mathbf{k}_2, \mathbf{k}_3). \quad (4.9)$$

On the right-hand side of the above formula, the first term $z_1^3\langle\delta h_{\mathbf{k}_1}\delta h_{\mathbf{k}_2}\delta h_{\mathbf{k}_3}\rangle$ is the three-point correlation function of the Higgs fluctuation $\delta h(\mathbf{k})$ generated by the self-interactions of Higgs field. The second term arises from replacing one $\delta h(\mathbf{k})$ by the nonlinear term $\frac{1}{2}z_2\delta h^2$, which exists even if the Higgs fluctuation $\delta h(\mathbf{k})$ is purely Gaussian.

As discussed in Section 2.1, the Higgs field could be treated as a massless scalar boson in de Sitter spacetime during inflation. Due to the SM Higgs self-interaction term, $\Delta\mathcal{L} = -(\lambda\bar{h})\delta h^3$, the three-point correlation function of δh is presented as the diagram of Fig. 5.

According to the Schwinger-Keldysh (SK) path integral formalism [49][50], we can compute the three-point correlation function of δh via following integral:

$$\begin{aligned} \langle\delta h_{\mathbf{k}_1}\delta h_{\mathbf{k}_2}\delta h_{\mathbf{k}_3}\rangle'(\tau_f) &= -i3!\lambda\bar{h}\int_{-\infty}^{\tau_f}d\tau a^4\left[\prod_{i=1}^3G_+(\mathbf{k}_i, \tau) - \prod_{i=1}^3G_-(\mathbf{k}_i, \tau)\right] \\ &= 12\lambda\bar{h}\text{Im}\left(\int_{-\infty}^{\tau_f}d\tau a^4\prod_{i=1}^3G_+(\mathbf{k}_i, \tau)\right), \end{aligned} \quad (4.10)$$

where λ is the SM Higgs self-coupling constant, \bar{h} is the uniform Higgs background during inflation, and the $G_{\pm}(\mathbf{k}_i, \tau)$ is the bulk-to-boundary propagator of massless scalar in the SK path integral defined in Appendix C. In Eq.(4.10), $\langle\delta h_{\mathbf{k}_1}\delta h_{\mathbf{k}_2}\delta h_{\mathbf{k}_3}\rangle'$ is defined as the three-point correlation function without including the delta function of momentum conservation, $\langle\delta h_{\mathbf{k}_1}\delta h_{\mathbf{k}_2}\delta h_{\mathbf{k}_3}\rangle = (2\pi)^3\delta^3(\mathbf{k}_1+\mathbf{k}_2+\mathbf{k}_3)\langle\delta h_{\mathbf{k}_1}\delta h_{\mathbf{k}_2}\delta h_{\mathbf{k}_3}\rangle'$. We derive the integral in the last line

of Eq.(4.10) to the leading order of τ_f as follows:

$$\begin{aligned}
& \text{Im} \left(\int_{-\infty}^{\tau_f} d\tau a^4 \prod_{i=1}^3 G_+(\mathbf{k}_i, \tau) \right) \\
&= \text{Im} \int_{-\infty}^{\tau_f} \frac{d\tau}{(H\tau)^4} \frac{H^6}{8k_1^3 k_2^3 k_3^3} \left(\prod_{i=1}^3 (1 - i k_i \tau) \right) e^{i(k_1+k_2+k_3)\tau} \\
&= \frac{H^2}{24k_1^3 k_2^3 k_3^3} \left\{ (k_1^3 + k_2^3 + k_3^3) \left[\ln(k_t |\tau_f|) + \gamma - \frac{4}{3} \right] + k_1 k_2 k_3 - \sum_{a \neq b} k_a^2 k_b \right\},
\end{aligned} \tag{4.11}$$

where $\gamma \simeq 0.577$ is the Euler-Mascheroni constant, and wavenumber $k_t = k_1 + k_2 + k_3$ is around the scale of the present observable universe. In the above correlation function, the leading contribution is given by the logarithmic term of $\ln(k_t |\tau_f|)$ and there is no inverse power term of $k_t |\tau_f|$ as proved in Ref. [49].

Thus, we further derive the three-point correlation function of δh as follows:

$$\begin{aligned}
\langle \delta h_{\mathbf{k}_1} \delta h_{\mathbf{k}_2} \delta h_{\mathbf{k}_3} \rangle' &= \frac{1}{2} \lambda \bar{h} H^2 \left\{ \left(\frac{1}{k_1^3 k_2^3} + 2 \text{perm.} \right) \left(-N_e + \gamma - \frac{4}{3} \right) \right. \\
&\quad \left. + \frac{1}{k_1^2 k_2^2 k_3^2} - \left(\frac{1}{k_1 k_2^2 k_3^3} + 5 \text{perm.} \right) \right\},
\end{aligned} \tag{4.12}$$

where N_e is the number of e-folds of the expansion from the time at which the fluctuation mode with momentum k_t first passed outside the horizon [$k_t^{-1} \simeq 1/(a_k H)$] until the end of inflation. The e-folding number N_e is derived as follows:

$$N_e = \ln \frac{a_{\text{end}}}{a_k} = \ln \frac{-(H\tau_f)^{-1}}{k_t/H} = -\ln(k_t |\tau_f|) \sim 60. \tag{4.13}$$

For the second term on the right-hand side of Eq.(4.9), it can be expressed as a four-point correlation function of δh , and to the leading order it is given by the product of two two-point correlation functions:

$$\begin{aligned}
z_1^2 z_2 \langle \delta h^4 \rangle(\mathbf{k}_1, \mathbf{k}_2, \mathbf{k}_3) &= \frac{z_1^2 z_2}{2} \int \frac{d^3 \mathbf{k}_0}{(2\pi)^3} \langle \delta h(\mathbf{k}_1) \delta h(\mathbf{k}_2) \delta h(\mathbf{k}_0) \delta h(\mathbf{k}_3 - \mathbf{k}_0) \rangle + (2 \text{ perm.}) \\
&= \frac{z_1^2 z_2}{2} \left[\int \frac{d^3 \mathbf{k}_0}{(2\pi)^3} \langle \delta h(\mathbf{k}_1) \delta h(\mathbf{k}_0) \rangle \langle \delta h(\mathbf{k}_2) \delta h(\mathbf{k}_3 - \mathbf{k}_0) \rangle + (\mathbf{k}_1 \leftrightarrow \mathbf{k}_2) \right] + (2 \text{ perm.}) \\
&= \frac{z_1^2 z_2}{2} \left[\int d^3 \mathbf{k}_0 (2\pi)^3 \delta^3(\mathbf{k}_1 + \mathbf{k}_0) \delta^3(\mathbf{k}_2 + \mathbf{k}_3 - \mathbf{k}_0) \frac{H^4}{4k_1^3 k_2^3} + (\mathbf{k}_1 \leftrightarrow \mathbf{k}_2) \right] + (2 \text{ perm.}) \\
&= (2\pi)^3 \delta^3(\mathbf{k}_1 + \mathbf{k}_2 + \mathbf{k}_3) z_1^2 z_2 \left[\frac{H^4}{4k_1^3 k_2^3} + (2 \text{ perm.}) \right].
\end{aligned} \tag{4.14}$$

Combining with the part arising from nonlinear rate, we derive the three-point correlation function of the comoving curvature perturbation ζ from Higgs-modulated reheating as follows:

$$\begin{aligned}
\langle \zeta_{\mathbf{k}_1} \zeta_{\mathbf{k}_2} \zeta_{\mathbf{k}_3} \rangle'_h &= \frac{z_1^3}{2} \lambda \bar{h} H^2 \left\{ \left[\frac{1}{k_1^3 k_2^3} + (2 \text{ perm.}) \right] \left(-N_e + \gamma - \frac{4}{3} \right) + \frac{1}{k_1^2 k_2^2 k_3^2} \right. \\
&\quad \left. - \left[\frac{1}{k_1 k_2^2 k_3^3} + (5 \text{ perm.}) \right] \right\} + \frac{z_1^2 z_2}{4} H^4 \left[\frac{1}{k_1^3 k_2^3} + (2 \text{ perm.}) \right].
\end{aligned} \tag{4.15}$$

In the above, we have included the non-Gaussianity contributions from both the nonlinear term and the Higgs self-interactions, whereas the previous studies only include the former [43–46].

4.3 Probing the Seesaw Scale through Local Non-Gaussianity

In the previous subsection, we derived the three-point correlation function $\langle \zeta_{\mathbf{k}_1} \zeta_{\mathbf{k}_2} \zeta_{\mathbf{k}_3} \rangle'_h$ for the curvature perturbation. For this subsection, we further compute the local non-Gaussianity $f_{\text{NL}}^{\text{local}}$ originating from the Higgs-modulated reheating in our model, with which we study the probe of seesaw mechanism.

The three-point correlation function $\langle \zeta_{\mathbf{k}_1} \zeta_{\mathbf{k}_2} \zeta_{\mathbf{k}_3} \rangle'_h$ contributes to three distinct classes of non-Gaussian shape templates (local, equilateral, and orthogonal types) according to Refs. [4][5]. We present a systematic analysis of the specific contributions of $\langle \zeta_{\mathbf{k}_1} \zeta_{\mathbf{k}_2} \zeta_{\mathbf{k}_3} \rangle'_h$ to these templates as in Appendix B. We evaluate the amplitude of a given non-Gaussian shape template, parameterized by f_{NL}^i , which is expressed as a function of the model parameters:

$$f_{\text{NL}}^i = f_{\text{NL}}^i(M, y_\nu, \lambda, H_{\text{inf}}, m_\phi, \Lambda), \quad (4.16)$$

where “ i ” represents the type of non-Gaussian shape template. For the present analysis, we choose a set of relevant parameters having benchmark values, as shown in Table 1. The amplitude of the comoving curvature perturbation power spectrum \mathcal{P}_ζ is taken as, $\ln(10^{10}\mathcal{P}_\zeta) \simeq 3.047$, according to the Planck-2018 data [3][48]. The SM Higgs self-coupling is set to be $\lambda = 0.001$.

Parameters	\mathcal{P}_ζ	N_e	H_{inf}	m_ϕ	Λ	λ
Values	2.1×10^{-9}	60	$(1, 3) \times 10^{13}$ GeV	$30H_{\text{inf}}$	$60H_{\text{inf}}$	0.001

Table 1. The relevant parameters with benchmark values chosen for the present analysis.

We find that the non-Gaussianity predicted by our model mainly belongs to the local type. This is due to the following reasons. First, in the three-point correlation function arising from the Higgs self-coupling, as described in Eq.(4.12), the local type is amplified by the number of e-folds N_e , whereas the other two shapes do not receive such enhancement. Second, as shown in Eq.(4.14), the contribution from the nonlinear term exclusively generates local-type non-Gaussianity. Hence, for the present study, we primarily focus on the magnitude of local non-Gaussianity (NG) as predicted by our model, which can be approximately expressed by the following:⁵

$$f_{\text{NL}}^{\text{local}} \simeq -\frac{10}{3} \frac{z_1^3 H^3}{(2\pi)^4 \mathcal{P}_\zeta^2} \left(\frac{\lambda \bar{h}}{2H} N_e - \frac{z_2 H}{4z_1} \right). \quad (4.17)$$

It is found that the local-type non-Gaussianity f_{NL} arising from the nonlinear term [43–45][47] is given by

$$f_{\text{NL}}^{\text{local}} = \frac{5z_2}{6z_1^2} = 5 \left(1 - \frac{\Gamma_0'' \Gamma_0}{\Gamma_0'^2} \right). \quad (4.18)$$

⁵The accurate formula is given in Eq.(B.5) of Appendix B.

Benchmark Points	A_1	A_2	B_1	B_2	C_1	C_2
Seesaw Scale (M/H_{inf})	2	2	5	5	10	10
Yukawa Coupling (y_ν)	0.3	0.6	0.3	0.6	0.3	0.6
$R = (\mathcal{P}_\zeta^{(h)}/\mathcal{P}_\zeta)^{1/2}$	0.04	0.17	0.06	0.23	0.05	0.19
$f_{\text{NL}}^{\text{local}}$ (Higgs self-coupling)	0.05	3.5	0.13	8.4	-0.08	-5.1
$f_{\text{NL}}^{\text{local}}$ (nonlinear term)	0.04	2.3	0.09	5.5	-0.05	-3.2
$f_{\text{NL}}^{\text{local}}$ (total)	0.09	5.7	0.22	14	-0.13	-8.3

Table 2. Comparison of major contributions to the non-Gaussianity arising from the Higgs self-interaction and the nonlinear term for three sets of benchmark points with specific neutrino seesaw scale M and the Higgs-neutrino Yukawa coupling y_ν . The ratio R of Eq.(3.19) is presented in the 4th row. The predicted values of $f_{\text{NL}}^{\text{local}}$ (Higgs self-coupling), $f_{\text{NL}}^{\text{local}}$ (nonlinear term) and $f_{\text{NL}}^{\text{local}}$ (total) are shown in the 5th, 6th and 7th rows, respectively.

We note that this result is compatible with the scenario where the Higgs fluctuation is the only source of primordial fluctuation, i.e., $R=1$. Besides, these studies assumed the absence of intrinsic non-Gaussianity in the Higgs field due to its self-coupling $\Delta\mathcal{L} = -(\lambda\bar{h})\delta h^3$, whose contribution however could be significant as will be shown below. For the present analysis, we incorporate both the intrinsic non-Gaussianity of the Higgs self-interactions and the nonlinear term. By assuming $R=1$ and purely Gaussian δh , our result will reduce to Eq.(4.18) as shown in Appendix B. But, in the general case, Eq.(4.17) includes two distinct contributions: one originating from the Higgs three-point correlation function induced by Higgs self-interactions, and another from the nonlinear term.

In the following, we will demonstrate that these contributions are comparable in magnitude for sample inputs of the Higgs self-coupling $\lambda=0.001$ and the e -folding $N_e=60$. For illustration, we give three sets of representative benchmark points where the seesaw scale is chosen as $M = (2, 5, 10)H_{\text{inf}}$ respectively; and for each given seesaw scale M we input the sample values of the Higgs-neutrino Yukawa coupling as $y_\nu = (0.3, 0.6)$ respectively. With these, we evaluate the contributions to the local non-Gaussianity $f_{\text{NL}}^{\text{local}}$ by the Higgs self-interaction and nonlinear term, which are presented and compared in Table 2 for the three sets of benchmark choices of the neutrino seesaw scale M and Yukawa coupling y_ν . This demonstrates that in the neutrino seesaw parameter space, the Higgs self-interaction can make a significant contribution to the non-Gaussianity and is comparable to the contribution of the nonlinear term.

In seesaw mechanism, the mass of the light left-handed neutrino ν is determined by the Majorana mass M and the neutrino-Higgs Yukawa coupling y_ν through the formula,

$$m_\nu = \frac{y_\nu^2 v^2}{2M} \sim O(0.05)\text{eV}, \quad (4.19)$$

where $v \simeq 246\text{GeV}$ is the vacuum expectation value of the Higgs field after electroweak symmetry breaking.⁶ The neutrino oscillation data give, $\Delta m_{13}^2 \simeq 2.5 \times 10^{-3} \text{eV}^2$ and $\Delta m_{12}^2 \simeq 7.4 \times 10^{-5} \text{eV}^2$ [19], which require at least one of the light neutrino masses to be $m_\nu \gtrsim$

⁶In Eq.(4.19), m_ν is the mass of the light neutrino ν at the electroweak scale. During and after the

0.05eV. With this, we can estimate the neutrino seesaw scale to be around 10^{14} GeV for the Yukawa coupling $y_\nu = O(1)$. On the other hand, cosmological measurements already impose nontrivial upper limits on the sum of the light neutrino masses which are around⁷ $\sum m_\nu \lesssim 0.1$ eV. This means that the scenario of normal ordering of light neutrino masses, the light neutrino mass could be as large as 0.1 eV, whereas for the case of inverted mass ordering there would be two neutrinos with masses around 0.05eV.

To probe the seesaw parameter space, we compute the non-Gaussianity $f_{\text{NL}}^{\text{local}}$ for different values of the seesaw scale M and neutrino-Higgs Yukawa coupling y_ν , where we set the SM Higgs self-coupling $\lambda = 0.001$. We present our findings numerically in Fig. 6. The colored region satisfies the requirement $R < 1$, whereas the uncolored region in the upper-right corner corresponds to $R \geq 1$. The region with blue color corresponds to $f_{\text{NL}}^{\text{local}} > 0$, whereas the red regions represent $f_{\text{NL}}^{\text{local}} < 0$.

As shown in Fig. 6, we find that the non-Gaussianity $f_{\text{NL}}^{\text{local}}$ has sign flip around the value of $M \simeq 9H_{\text{inf}}$. This can be understood as follows. We note that in the parameter space considered in this study, the sign of the non-Gaussianity is mainly determined by the contribution from the Higgs self-interaction. As shown in Eq.(4.17), it is linked to the coefficient z_1 , which depends on the derivative of the inflaton decay width. Since the Higgs during inflation enters the decay width through the neutrino seesaw as shown in Eq.(3.3), the derivative $\Gamma'_0 = d\Gamma_{\text{reh}}/dh_{\text{inf}}$ is given by

$$\Gamma'_0 = \frac{d\Gamma_{\text{reh}}}{dM_N} \frac{dM_N}{dh_{\text{inf}}}, \quad (4.20)$$

where $\Gamma'_0 \propto z_1$ according to Eq.(4.4) and the derivative $\frac{dM_N}{dh_{\text{inf}}} \simeq \frac{y_\nu^2 h_{\text{reh}}}{M^2} \frac{dh_{\text{reh}}}{dh_{\text{inf}}}$ is nonzero. Hence the condition $z_1 = 0$ requires $\frac{d\Gamma_{\text{reh}}}{dM_N} = 0$. At the time of reheating, we have $M_N \simeq M$, at which we compute the derivative:

$$\frac{d\Gamma_{\text{reh}}}{dM_N} = \frac{m_\phi M}{8\pi\Lambda^2} \left[\left(1 - \frac{M^2}{m_\phi^2}\right)^2 \left(1 - \frac{4M^2}{m_\phi^2}\right)^{\frac{1}{2}} - \frac{8M^2}{m_\phi^2} \right] \left(1 - \frac{4M^2}{m_\phi^2}\right)^{-\frac{1}{2}}. \quad (4.21)$$

From the condition $\frac{d\Gamma_{\text{reh}}}{dM_N} = 0$, we solve the ratio of the seesaw scale M over the inflaton mass m_ϕ as follows:

$$\frac{M}{m_\phi} \simeq 0.29. \quad (4.22)$$

Thus, for the input of $m_\phi = 30H_{\text{inf}}$, the sign-transition point $z_1 = 0$ corresponds to $M \simeq 8.7H_{\text{inf}}$. This nicely explains that the transition between $f_{\text{NL}}^{\text{local}} > 0$ and $f_{\text{NL}}^{\text{local}} < 0$ in Fig. 6 happens around the horizontal line of $M \simeq 9H_{\text{inf}}$.

In Fig. 6, the green curve describes the existing 2σ limits, $-11.1 \leq f_{\text{NL}}^{\text{local}} \leq 9.3$, as given by the Planck-2018 data [4]. Moreover, we display contours for $f_{\text{NL}} = \pm 1, \pm 0.1, \pm 0.01$,

inflation, we can include the renormalization-group (RG) running effect for this neutrino mass at the corresponding Hubble scale of $O(10^{13})$ GeV, which is about 30% larger than its low energy value at the electroweak scale [51][52].

⁷For instance, the eBOSS Collaboration [53] placed a 95% upper bound $\sum m_\nu \lesssim 0.10$ eV and the DES Collaboration [54] set a constraint $\sum m_\nu \lesssim 0.13$ eV at 95% C.L.

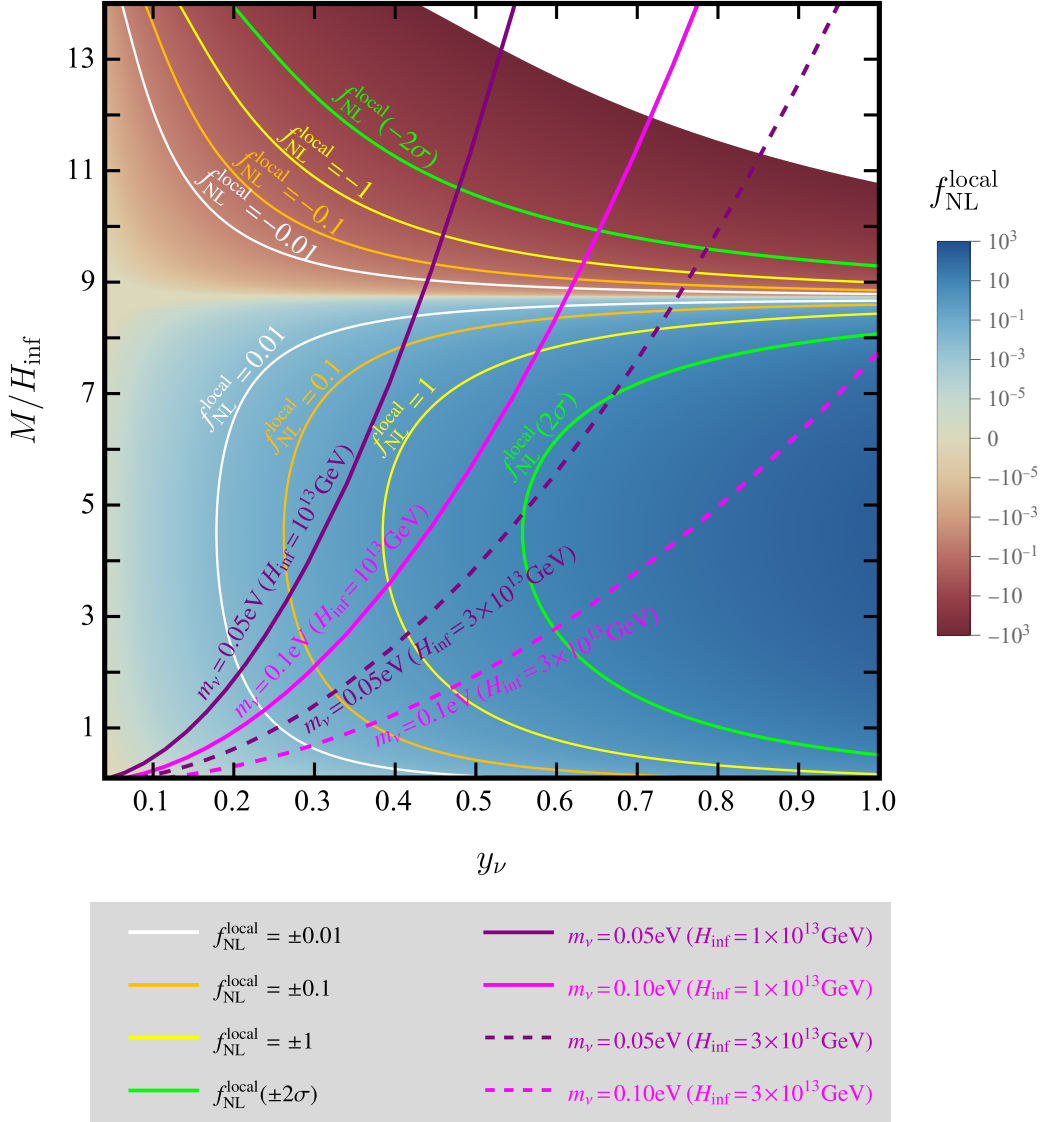


Figure 6. Prediction of the non-Gaussianity $f_{\text{NL}}^{\text{local}}$ from the seesaw parameter space of heavy neutrino mass scale M versus Yukawa coupling y_ν , where the SM Higgs self-coupling is input as $\lambda = 0.001$, and the Hubble parameter during inflation is set as $H_{\text{inf}} = 10^{13}\text{GeV}$ and $3 \times 10^{13}\text{GeV}$, respectively. The blue region represents the parameter space with positive $f_{\text{NL}}^{\text{local}}$, whereas the red region represents the parameter space with negative $f_{\text{NL}}^{\text{local}}$. The green contour depicts the 2σ bound based on Planck-2018 data, corresponding to $-11.1 \leq f_{\text{NL}}^{\text{local}} \leq 9.3$. The colored region satisfies the requirement of $R < 1$ and the uncolored region in the upper-right corner corresponds to $R \geq 1$.

plotted as yellow, orange, and white curves, respectively. These contours represent the potential sensitivity reaches of the ongoing and future observations, such as those from DESI [55], CMB-S4 [56], Euclid [57], SPHEREx [58], LSST [59], and SKA [60] experiments. We present the seesaw predictions for the light neutrino mass of $m_\nu = 0.1\text{eV}$ (pink curves) and $m_\nu = 0.05\text{eV}$ (purple curves), and for the Hubble parameter $H = 10^{13}\text{GeV}$ (solid curves)

and $H = 3 \times 10^{13} \text{ GeV}$ (dashed curves), where we have included the renormalization-group running effects for the light neutrino mass at the Hubble scale. It shows that a larger value of the Hubble parameter will shift the pink and purple curves towards the right-hand-side region with larger Yukawa coupling y_ν .

For the local-type non-Gaussianity (NG) $f_{\text{NL}}^{\text{local}} > 0$, we see that the existing measurements of Planck-2018 (shown as the 2σ green contour) already have sensitivity to probe the case of a light neutrino mass around $m_\nu = 0.05 \text{ eV}$ for Hubble parameter $H = 3 \times 10^{13} \text{ GeV}$, as shown by the purple dashed curve; whereas for a larger light neutrino mass around $m_\nu = 0.1 \text{ eV}$ with $H = 3 \times 10^{13} \text{ GeV}$, a large portion of the parameter region is already excluded by the Planck-2018 data as shown by the pink dashed curve. Then, for a smaller Hubble parameter $H = 10^{13} \text{ GeV}$, Fig. 6 shows that for inputting the light neutrino mass of range $m_\nu = (0.05 - 0.1) \text{ eV}$, our seesaw predictions (purple and pink solid curves) are consistent with the current bound of Planck-2018 (shown as the 2σ green contour); but they can be further probed by the improved non-Gaussianity measurements of future experiments as shown by the (yellow, orange, white) contours. For instance, probing the case of a light neutrino mass $m_\nu = 0.05 \text{ eV}$ and Hubble parameter $H = 10^{13} \text{ GeV}$ (purple solid curve) requires a sensitivity to $f_{\text{NL}}^{\text{local}} \sim 0.1$ or even $f_{\text{NL}}^{\text{local}} \sim 0.01$, depending on the seesaw mass scale M . In contrast, the case of $m_\nu = 0.1 \text{ eV}$ (pink solid curve) appears more promising for detection in the near future.

In parallel, for the case of $f_{\text{NL}}^{\text{local}} < 0$, Fig. 6 shows that the existing bounds of Planck-2018 measurements (shown as the -2σ green contour) have already excluded a large portion of the seesaw parameter space. For instance, for a light neutrino mass $m_\nu = 0.1 \text{ eV}$ (0.05 eV) and Hubble parameter $H = 10^{13} \text{ GeV}$, the parameter space with seesaw scale $M \gtrsim 10H_{\text{inf}}$ ($M \gtrsim 11H_{\text{inf}}$) is excluded by the Planck-2018 data. The future measurements of non-Gaussianity under planning will be able to extensively probe the seesaw parameter space with $M \gtrsim 9H_{\text{inf}}$ in the case of $f_{\text{NL}}^{\text{local}} < 0$.

Finally, as shown by Fig. 6 the cosmological non-Gaussianity measurements are rather sensitive to the value of light neutrino mass scale m_ν which is constrained by the low energy neutrino experiments, especially the determination of the light neutrino mass ordering (as will be given by the neutrino oscillation experiments such as JUNO [61] and DUNE [62]). Hence, our analysis of Fig. 6 demonstrates the important interplay between the light neutrino mass determination by the low energy experiments (including the neutrino mass ordering determination as well as pinning down the Majorana nature of light neutrinos by the neutrinoless double-beta decay experiments [63]) and the high-scale cosmological measurements on non-Gaussianity.

In passing, we comment on the effect of Λ and m_ϕ on our results. These parameters can affect the time of reheating completion t_{reh} . For a larger m_ϕ or a smaller Λ , inflaton decays earlier, allowing less time for Higgs field value to decrease as shown in Eq.(2.20) and causing larger fluctuations, thereby increasing the non-Gaussianity. Hence, further understanding on the UV dynamics of inflation for the determinations of H_{inf} , m_ϕ and Λ will be beneficial for definitive probe of the seesaw parameter space. Besides, in the future work we can further extend the seesaw mechanism to include all three generations

of neutrinos, with which the neutrino mixing angles and CP phases may be probed through the non-Gaussianity measurements.

5 Conclusions

Seesaw mechanism provides the most appealing resolution to the origin of tiny masses of active neutrinos. But the natural seesaw scale is as high as 10^{14} GeV, posing a great challenge for experimental tests at particle colliders. Given the striking fact that the neutrino seesaw scale align with the inflation scale, we proposed in this work a framework incorporating inflation and neutrino seesaw in which the inflaton primarily decays into heavy right-handed neutrinos. The inflaton couples to the right-handed neutrinos through an effective interaction that respects the shift symmetry. Through the neutrino seesaw, fluctuations of the Higgs field can modulate the inflaton decay, leading to non-Gaussian signatures at large scales. This provides an important means to directly probe the seesaw mechanism in the early universe. Moreover, it is really appealing that this scenario also naturally provides an initial setup for the leptogenesis of matter-antimatter asymmetry where sufficient right-handed neutrinos are generated after reheating. This approach further provides a new framework of the cosmological Higgs collider, in which the Higgs modulated reheating is naturally realized by the inflaton decays into right-handed neutrinos within neutrino seesaw.

In Section 2, we studied the dynamics and evolution of the Higgs field during and after inflation. During the inflation, large quantum fluctuations of the Higgs field are generated due to the high scale of inflation $H_{\text{inf}} = O(10^{13} - 10^{14})$ GeV. If the inflation lasts long enough, the distribution of Higgs field would finally reach an equilibrium state and the average of Higgs field takes a value around the Hubble scale, as shown in Eq.(2.16). After inflation, the value of Higgs field $h(t)$ would oscillate and decrease. We also gave a semi-analytic formula (2.20) for the evolution of the Higgs field $h(t)$ after inflation, which fits well with the exact numerical calculations as demonstrated in Fig. 3.

In Section 3, we presented an approach that incorporates both the inflation and neutrino seesaw mechanism. The inflaton ϕ and the right-handed neutrino N_R are both the SM singlets, and they couple together through a unique dimension-5 operator as in Eq.(3.1) that respects the shift symmetry. In this approach, the inflaton primarily decays into right-handed neutrinos after inflation. With the neutrino seesaw mechanism, the Higgs field can influence the reheating process through the modulation of inflaton decays into right-handed neutrinos. In consequence, the curvature perturbations are generated by fluctuations in the Higgs field. We established a relation (3.12) between the curvature perturbations and the Higgs fluctuations, as illustrated in Fig. 4. A further expanded formula for this relation up to $O(\delta h_{\text{inf}}^2)$ is given in Eq.(4.1).

In Section 4, we investigated the primordial local non-Gaussianity arising from the Higgs-modulated reheating through the inflaton decays into right-handed neutrinos within seesaw mechanism. We demonstrated that our method provides observable signatures of primordial non-Gaussianity, which can be used to probe the neutrino seesaw mechanism. We performed a full analysis for the two-point and three-point correlation functions of

the comoving curvature perturbation ζ_h as contributed by the Higgs fluctuations in our model. We found that the primordial non-Gaussianity is contributed by both the Higgs self-interaction and the nonlinear term, which are comparable and the former was not considered in the literature. We presented the predictions for the local non-Gaussianity $f_{\text{NL}}^{\text{local}}$ from the parameter space of neutrino seesaw, as shown in Fig. 6. We found that for a fairly modest value of Higgs self-coupling, a sensitivity to the non-Gaussian signatures of $f_{\text{NL}}^{\text{local}} = O(1)$ could probe the seesaw scale $M \sim 10^{13}$ GeV. In the near future, combining the neutrino data (such as those from the JUNO [61] and DUNE [62] experiments) with the improved non-Gaussianity measurements (such as those from DESI [55], CMB-S4 [56], Euclid [57], SPHEREx [58], LSST [59], and SKA [60] experiments) is expected to provide more sensitive probe on the neutrino seesaw parameter space. The main idea and results of this work are summarized in the companion letter paper [64].

Acknowledgments

We thank Misao Sasaki, Zhong-Zhi Xianyu, and Yi Wang for useful discussions. The research of HJH, LS and JY was supported in part by the National Natural Science Foundation of China under grants 12175136 and 11835005. C.H. acknowledges supports from the Sun Yat-Sen University Science Foundation, the Fundamental Research Funds for the Central Universities at Sun Yat-sen University under Grant No. 24qnpy117, the National Key R&D Program of China under grant 2023YFA1606100, and the Key Laboratory of Particle Astrophysics and Cosmology (MOE) of Shanghai Jiao Tong University.

Appendix

A Evolution of Higgs Field after Inflation

In this Appendix, we provide further technical derivations for the evolution of Higgs field after inflation to support the analysis of Section 2. For the sake of convenience, we rescale all physical quantities according to their dimensions by the Hubble parameter H_{inf} during the inflation. Thus, they become dimensionless under the following rescaling:⁸

$$h \rightarrow \left(\frac{3}{2}H_{\text{inf}}\right)h, \quad t \rightarrow \left(\frac{3}{2}H_{\text{inf}}\right)^{-1}t, \quad \dot{h} \rightarrow \left(\frac{3}{2}H_{\text{inf}}\right)^2\dot{h}. \quad (\text{A.1})$$

After inflation and before the completion of reheating, we assume the universe is matter-dominated. Hence, the scale factor $a(t)$ and the Hubble parameter $H(t)$ take the following forms:

$$a(t) = \left(\frac{t}{t_0}\right)^{2/3}, \quad H(t) = \frac{2}{3t}, \quad (\text{A.2})$$

where t_0 represents the initial time of matter domination, and the Hubble parameter at t_0 satisfies $H(t_0) = \frac{2}{3t_0} = H_{\text{inf}}$. The equation of motion for the Higgs field $h(t)$ is given by

$$\ddot{h}(t) + \frac{2}{t}\dot{h}(t) + \lambda h^3(t) = 0. \quad (\text{A.3})$$

⁸In this rescaling, we have also included a numerical factor $\frac{3}{2}$ for convenience, such that the initial time t_0 defined below Eq.(A.2) will simply become $t_0 = 1$.

We can define the conformal time τ during the matter-dominated stage as follows:

$$\tau = \int \frac{dt}{a(t)} = 3t^{1/3}. \quad (\text{A.4})$$

The definition of conformal time used here differs from that used in the calculation of correlation functions. During inflation, conformal time is always negative, with values approaching zero which corresponds to an infinitely distant future. But, in the present context of a different cosmic expansion, conformal time is positive. These two definitions can be related by a simple constant shift. Thus, we can express the scale factor a in terms of conformal time τ as $a(\tau) = \frac{1}{9}\tau^2$. Based on this conformal time, we define

$$\begin{aligned} \varphi &\equiv ah = t^{2/3}h = \frac{1}{9}\tau^2h, \\ \varphi' &\equiv \frac{d\varphi}{d\tau}, \quad \varphi'' \equiv \frac{d^2\varphi}{d\tau^2}, \\ a' &\equiv \frac{da}{d\tau}, \quad a'' \equiv \frac{d^2a}{d\tau^2}. \end{aligned} \quad (\text{A.5})$$

For the following derivations, we will use the two relations involving derivatives of the scale factor a :

$$\frac{a'}{a} = \frac{2}{\tau}, \quad \frac{a''}{a} = \frac{2}{\tau^2}. \quad (\text{A.6})$$

We then obtain the equation of motion for the redefined field $\varphi(\tau)$,

$$\varphi''(\tau) - \frac{a''}{a}\varphi(\tau) + \lambda\varphi(\tau)^3 = 0. \quad (\text{A.7})$$

For a quantity A , we denote A_0 as $A(t = t_0) = A(\tau = \tau_0)$, where t_0 and τ_0 denote the initial physical time and its corresponding conformal time respectively. We set the initial conditions as follows:

$$\begin{aligned} t_0 = 1, \quad \tau_0 = 3, \quad a_0 = 1, \\ h_0 = h_{\text{inf}}, \quad \dot{h}_0 = 0, \quad \varphi_0 = h_0, \quad \varphi'_0 = \frac{2}{3}h_0. \end{aligned} \quad (\text{A.8})$$

In the above, $t_0 = 1$ implies $H(t_0) = H_{\text{inf}}$ and h_0 is the initial value of $h(t)$ which is determined at the end of inflation. We take $h_0 > 0$ as an example for the following calculation, but the results can be readily generalized to the case of $h_0 < 0$. When the conformal time is small, the term $-\frac{2}{\tau^2}\varphi$ dominates, and the other term $\lambda\varphi^3$ can be neglected for small λ . Hence, we could first solve the following equation,

$$\varphi'' - \frac{2}{\tau^2}\varphi = 0, \quad (\text{A.9})$$

with the initial conditions $\varphi_0 = h_0$ and $\varphi'_0 = \frac{2}{3}h_0$. We thus derive the following solution:

$$\varphi(\tau) = \frac{1}{9}h_0\tau^2. \quad (\text{A.10})$$

As the conformal time increases, the term $\lambda\varphi^3$ becomes increasingly significant. When $\lambda\varphi(\tau)^3 = \frac{2}{\tau^2}\varphi(\tau)$, we identify the conformal time cutoff τ_{cut} as follows:

$$\tau_{\text{cut}} = 3^{2/3}2^{1/6}\lambda^{-1/6}h_0^{-1/3}. \quad (\text{A.11})$$

Then, we deduce $\varphi_{\text{cut}} \equiv \varphi(\tau_{\text{cut}}) = \frac{1}{9}h_0\tau_{\text{cut}}^2$ and $\varphi'_{\text{cut}} \equiv \varphi'(\tau_{\text{cut}}) = \frac{2}{9}h_0\tau_{\text{cut}}$. Note that the solution (A.10) is valid when $\tau \leq \tau_{\text{cut}}$.

At the late-time stage $\tau \gg \tau_{\text{cut}}$, the term $\lambda\varphi^3$ dominates and the term $-\frac{2}{\tau^2}\varphi$ may be neglected. In consequence, we simplify Eq.(A.7) as follows:

$$\varphi''(\tau) + \lambda\varphi^3(\tau) = 0. \quad (\text{A.12})$$

We can define a conserved quantity as the conformal ‘‘energy’’:

$$\frac{1}{2}\varphi'^2 + \frac{\lambda}{4}\varphi^4 = E, \quad (\text{A.13})$$

where we could define $E_K = \frac{1}{2}\varphi'^2$ as the conformal kinematic energy and $E_V = \frac{\lambda}{4}\varphi^4$ as the conformal potential energy. This equation implies that the field φ oscillates within the potential $\frac{\lambda}{4}\varphi^4$ without attenuation or damping. The solution to Eq.(A.12) is given by an elliptic sine function, which can be approximated as follows:

$$\varphi(\tau) = \varphi_{\text{max}} \cos\left[\frac{\Gamma^2(3/4)}{\sqrt{\pi}}\sqrt{\lambda}\varphi_{\text{max}}(\tau - \tau_{\text{cut}}) + \theta\right], \quad (\text{A.14})$$

where φ_{max} is the oscillation amplitude and θ is the phase, both of which are determined by initial conditions. Matching the ‘‘energy’’ at the time τ_{cut} , we could determine the phase θ and the oscillation amplitude φ_{max} :

$$\begin{cases} \frac{E_K}{E_V} = 4 = \tan^2\theta, \\ E = E_K + E_V = \frac{5\lambda}{4}\varphi_{\text{cut}}^4 = \frac{\lambda}{4}\varphi_{\text{max}}^4, \end{cases} \implies \begin{cases} \theta = -\arctan 2 \simeq -1.1, \\ \varphi_{\text{max}} = 2^{1/3}3^{-2/3}5^{1/4}\left(\frac{h_0}{\lambda}\right)^{1/3}. \end{cases} \quad (\text{A.15})$$

Then, we derive an analytic solution as a piecewise function:

$$\varphi(\tau) = \begin{cases} \frac{1}{9}h_0\tau^2, & \tau \leq \tau_{\text{cut}}, \\ \varphi_{\text{max}} \cos\left[\frac{\Gamma^2(3/4)}{\sqrt{\pi}}\sqrt{\lambda}\varphi_{\text{max}}(\tau - \tau_{\text{cut}}) + \theta\right], & \tau > \tau_{\text{cut}}. \end{cases} \quad (\text{A.16})$$

With these, we derive the solution of Higgs field $h(t)$ in terms of physical time t as follows:

$$h(t) = \frac{\varphi(3t^{1/3})}{a(t)} = \begin{cases} h_0, & t \leq t_{\text{cut}}, \\ A\left(\frac{h_0}{\lambda}\right)^{1/3}t^{-2/3} \cos\left[\lambda^{1/6}h_0^{1/3}\omega(t^{1/3} - t_{\text{cut}}^{1/3}) + \theta\right], & t > t_{\text{cut}}, \end{cases} \quad (\text{A.17})$$

where $t_{\text{cut}} = \left(\frac{1}{3}\tau_{\text{cut}}\right)^3$, and the coefficients A and ω are given by

$$A = 2^{1/3}3^{-2/3}5^{1/4} \simeq 0.9, \quad (\text{A.18a})$$

$$\omega = \frac{\Gamma^2(3/4)}{\sqrt{\pi}} 2^{1/3} 3^{1/3} 5^{1/4} \simeq 2.3. \quad (\text{A.18b})$$

Using the definition of τ_{cut} in Eq.(A.11), we could convert the term $\lambda^{1/6} h_0^{1/3} \omega t_{\text{cut}}^{1/3}$ of Eq.(A.17) into a constant phase:

$$\lambda^{1/6} h_0^{1/3} \omega t_{\text{cut}}^{1/3} = \frac{1}{3} \lambda^{1/6} h_0^{1/3} \omega \tau_{\text{cut}} = 3^{-1/3} 2^{1/6} \omega. \quad (\text{A.19})$$

Finally, we further derive Eq.(A.17) as follows:

$$h(t) = \begin{cases} h_0, & t \leq t_{\text{cut}}, \\ A \left(\frac{h_0}{\lambda} \right)^{1/3} t^{-2/3} \cos \left[\lambda^{1/6} h_0^{1/3} \omega t^{1/3} + \theta' \right], & t > t_{\text{cut}}, \end{cases} \quad (\text{A.20})$$

where the phase $\theta' = -\lambda^{1/6} h_0^{1/3} \omega t_{\text{cut}}^{1/3} + \theta \simeq -2.9$. Recall that we employ the factor $\frac{3}{2} H_{\text{inf}}$ to define dimensionless physical quantities in Eq.(A.1). We can recover the dimensions of relevant physical variables by the following rescaling:

$$\begin{aligned} t &\rightarrow \left(\frac{3}{2} H_{\text{inf}} \right) t, & t_0 &\rightarrow \left(\frac{3}{2} H_{\text{inf}} \right) t_0, & t_{\text{cut}} &\rightarrow \left(\frac{3}{2} H_{\text{inf}} \right) t_{\text{cut}}, \\ h(t) &\rightarrow h(t) / \left(\frac{3}{2} H_{\text{inf}} \right), & h_0 &\rightarrow h_0 / \left(\frac{3}{2} H_{\text{inf}} \right), \end{aligned} \quad (\text{A.21})$$

under which the form of the formula (A.20) remains unchanged.

B Derivation of Non-Gaussianity

The Planck collaboration gives a list of primordial non-Gaussianity measurements with various shapes [4]. For the present study, we will use the shape templates of local-type, equilateral-type, and orthogonal-type non-Gaussianity measurements.

For the local-type non-Gaussianity, we compute the three-point correlation function:

$$\begin{aligned} \langle \Phi_{\mathbf{k}_1} \Phi_{\mathbf{k}_2} \Phi_{\mathbf{k}_3} \rangle'_{\text{local}} &= B_{\Phi}^{\text{local}}(k_1, k_2, k_3) \\ &= 2A^2 f_{\text{NL}}^{\text{local}} \left(\frac{1}{k_1^3 k_2^3} + \frac{1}{k_2^3 k_3^3} + \frac{1}{k_3^3 k_1^3} \right) \equiv 2A^2 f_{\text{NL}}^{\text{local}} F^{\text{local}}(k_1, k_2, k_3), \end{aligned} \quad (\text{B.1})$$

where Φ denotes the Bardeen gravitational potential, which is related to the comoving curvature perturbation ζ via $\Phi \equiv \frac{3}{5} \zeta$ on superhorizon scales. The power spectrum $P_{\Phi} = \langle \Phi_{\mathbf{k}_1} \Phi_{\mathbf{k}_2} \rangle'$ is given by $P_{\Phi} = A/k^3$, where A is the normalization constant. Given $\Phi = \frac{3}{5} \zeta$ and $P_{\Phi} = \langle \Phi_{\mathbf{k}_1} \Phi_{\mathbf{k}_2} \rangle' = A/k^3$ (under the approximation $n_s \simeq 1$), we derive the normalization constant $A = 2\pi^2 \left(\frac{3}{5} \right)^2 P_{\zeta}$. In the above formula and hereafter, we have defined $\langle \Phi_{\mathbf{k}_1} \Phi_{\mathbf{k}_2} \Phi_{\mathbf{k}_3} \rangle'$ as the 3-point correlation function without including the delta function of momentum conservation, $\langle \Phi_{\mathbf{k}_1} \Phi_{\mathbf{k}_2} \Phi_{\mathbf{k}_3} \rangle = (2\pi)^3 \delta^3(\mathbf{k}_1 + \mathbf{k}_2 + \mathbf{k}_3) \langle \Phi_{\mathbf{k}_1} \Phi_{\mathbf{k}_2} \Phi_{\mathbf{k}_3} \rangle'$.

For the equilateral-type non-Gaussianity, the three-point correlation function is computed as follows:

$$\begin{aligned} \langle \Phi_{\mathbf{k}_1} \Phi_{\mathbf{k}_2} \Phi_{\mathbf{k}_3} \rangle'_{\text{equil}} &= B_{\Phi}^{\text{equil}}(k_1, k_2, k_3) \\ &= 6A^2 f_{\text{NL}}^{\text{equil}} \left[-\frac{1}{k_1^3 k_2^3} - \frac{1}{k_2^3 k_3^3} - \frac{1}{k_3^3 k_1^3} - \frac{2}{(k_1 k_2 k_3)^2} + \left(\frac{1}{k_1 k_2^2 k_3^3} + 5 \text{ perm.} \right) \right] \\ &\equiv 6A^2 f_{\text{NL}}^{\text{equil}} F^{\text{equil}}(k_1, k_2, k_3). \end{aligned} \quad (\text{B.2})$$

For the orthogonal-type non-Gaussianity, we can derive the three-point correlation function as follows:

$$\begin{aligned}
\langle \Phi_{\mathbf{k}_1} \Phi_{\mathbf{k}_2} \Phi_{\mathbf{k}_3} \rangle'_{\text{ortho}} &= B_{\Phi}^{\text{ortho}}(k_1, k_2, k_3) \\
&= 6A^2 f_{\text{NL}}^{\text{ortho}} \left[-\frac{3}{k_1^3 k_2^3} - \frac{3}{k_2^3 k_3^3} - \frac{3}{k_3^3 k_1^3} - \frac{8}{(k_1 k_2 k_3)^2} + \left(\frac{3}{k_1 k_2^2 k_3^3} + 5 \text{ perm.} \right) \right] \\
&\equiv 6A^2 f_{\text{NL}}^{\text{ortho}} F^{\text{ortho}}(k_1, k_2, k_3).
\end{aligned} \tag{B.3}$$

Next, we can use the above templates to analyze a three-point correlation function of the curvature perturbation $\langle \zeta_{\mathbf{k}_1} \zeta_{\mathbf{k}_2} \zeta_{\mathbf{k}_3} \rangle'$ through

$$\begin{aligned}
\langle \Phi_{\mathbf{k}_1} \Phi_{\mathbf{k}_2} \Phi_{\mathbf{k}_3} \rangle' &= \left(\frac{3}{5} \right)^3 \langle \zeta_{\mathbf{k}_1} \zeta_{\mathbf{k}_2} \zeta_{\mathbf{k}_3} \rangle' \\
&= 2A^2 \left[f_{\text{NL}}^{\text{local}} F^{\text{local}}(k_1, k_2, k_3) + 3f_{\text{NL}}^{\text{equil}} F^{\text{equil}}(k_1, k_2, k_3) + 3f_{\text{NL}}^{\text{ortho}} F^{\text{ortho}}(k_1, k_2, k_3) \right],
\end{aligned} \tag{B.4}$$

where $F^{\text{local}}(k_1, k_2, k_3)$, $F^{\text{equil}}(k_1, k_2, k_3)$, and $F^{\text{ortho}}(k_1, k_2, k_3)$ are functions of the external momenta (k_1, k_2, k_3) . In the present analysis, we find that the three-point correlation function $\langle \zeta_{\mathbf{k}_1} \zeta_{\mathbf{k}_2} \zeta_{\mathbf{k}_3} \rangle'$ can be expressed as the sum of these three shape templates with relevant coefficients f_{NL} .

We can directly solve the coefficients f_{NL} as follows:

$$f_{\text{NL}}^{\text{equil}} = \frac{5}{12} P, \quad f_{\text{NL}}^{\text{ortho}} = -\frac{1}{12} P, \quad f_{\text{NL}}^{\text{local}} = \frac{1}{2} [P(N_e - \gamma + \frac{7}{3}) + Q], \tag{B.5}$$

where the quantities P and Q are given by

$$P = -\frac{20z_1^3 H^3}{3(2\pi)^4 P_\zeta^2} \frac{\lambda \bar{h}}{2H}, \tag{B.6a}$$

$$Q = \frac{20z_1^3 H^3}{3(2\pi)^4 P_\zeta^2} \frac{z_2 H}{4z_1}. \tag{B.6b}$$

We may also compare our results with the literature [43–45][47] which considered the special case of $R = 1$ and ignored the contribution from Higgs self-coupling. In this case, given $R = |z_1| (P_{\delta h} / P_\zeta)^{1/2}$, we obtain $(P_{\delta h} / P_\zeta)^{1/2} = R / |z_1|$. Under the assumption that Higgs fluctuation δh is scale invariant, i.e., $P_{\delta h}^{1/2} = H / (2\pi)$, we deduce the following result:

$$f_{\text{NL}}^{\text{local}} = \frac{Q}{2} = \frac{5z_1^3 H^3}{6(2\pi)^4 P_\zeta^2} \frac{z_2 H}{z_1} = \frac{5}{6} \frac{P_{\delta h}^2}{P_\zeta^2} z_1^2 z_2 = R^4 \frac{5z_2}{6z_1^2}. \tag{B.7}$$

Using $z_1 = -\Gamma'_0 / (6\Gamma_0)$ and $z_2 = -(\Gamma_0 \Gamma''_0 - \Gamma'_0 \Gamma'_0) / (6\Gamma_0^2)$ as defined in Section 4.1, and the condition that $R = 1$, we thus derive the local non-Gaussianity,

$$f_{\text{NL}}^{\text{local}} = \frac{5z_2}{6z_1^2} = 5 \left(1 - \frac{\Gamma''_0 \Gamma_0}{(\Gamma'_0)^2} \right), \tag{B.8}$$

which agrees with the literature [43–45][47].

C Schwinger-Keldysh Propagators of Higgs Field

The Klein-Gordon equation in de Sitter spacetime for the massless scalar field is given by

$$\square u_{\mathbf{k}} = \ddot{u}_{\mathbf{k}} + 3H\dot{u}_{\mathbf{k}} + \frac{\mathbf{k}^2}{a^2(t)}u_{\mathbf{k}} = 0, \quad (\text{C.1})$$

where $H = \dot{a}/a$ is constant and $a(t) = e^{Ht}$. We may consider the conformal coordinates with $d\tau = dt/a(\tau)$ and $a = -(H\tau)^{-1}$, and re-express the Klein-Gordon equation as follows:

$$u_{\mathbf{k}}'' - \frac{2}{\tau}u_{\mathbf{k}}' + \mathbf{k}^2u_{\mathbf{k}} = 0. \quad (\text{C.2})$$

The normalized mode function of the massless scalar field in de Sitter spacetime with the Bunch-Davis vacuum can be solved as

$$u_{\mathbf{k}}(\tau) = \frac{H}{\sqrt{2k^3}}(1 + ik\tau)e^{-ik\tau}, \quad (\text{C.3})$$

where we denote $u' = du/d\tau$ and $u'' = d^2u/d\tau^2$.

In the Schwinger-Keldysh (SK) path integral formalism, the bulk-to-bulk propagators are defined as follows:

$$G_{++}(\mathbf{k}; \tau_1, \tau_2) = G_{>}(\mathbf{k}; \tau_1, \tau_2)\theta(\tau_1 - \tau_2) + G_{<}(\mathbf{k}; \tau_1, \tau_2)\theta(\tau_2 - \tau_1), \quad (\text{C.4a})$$

$$G_{+-}(\mathbf{k}; \tau_1, \tau_2) = G_{<}(\mathbf{k}; \tau_1, \tau_2), \quad (\text{C.4b})$$

$$G_{-+}(\mathbf{k}; \tau_1, \tau_2) = G_{>}(\mathbf{k}; \tau_1, \tau_2), \quad (\text{C.4c})$$

$$G_{--}(\mathbf{k}; \tau_1, \tau_2) = G_{<}(\mathbf{k}; \tau_1, \tau_2)\theta(\tau_1 - \tau_2) + G_{>}(\mathbf{k}; \tau_1, \tau_2)\theta(\tau_2 - \tau_1), \quad (\text{C.4d})$$

where we have defined,

$$G_{>}(\mathbf{k}; \tau_1, \tau_2) = u_{\mathbf{k}}(\tau_1)u_{\mathbf{k}}^*(\tau_2) = \frac{H^2}{2k^3} [1 + ik(\tau_1 - \tau_2) + k^2\tau_1\tau_2]e^{-ik(\tau_1 - \tau_2)}, \quad (\text{C.5a})$$

$$G_{<}(\mathbf{k}; \tau_1, \tau_2) = u_{\mathbf{k}}^*(\tau_1)u_{\mathbf{k}}(\tau_2) = G_{>}^*(\mathbf{k}; \tau_1, \tau_2). \quad (\text{C.5b})$$

Besides, the bulk-to-boundary propagator is a special propagator in which external legs terminated at the final slice, i.e., $\tau = \tau_f \rightarrow 0^-$,

$$G_{\pm}(\mathbf{k}, \tau) = G_{\pm+}(\mathbf{k}; \tau, \tau_f), \quad (\text{C.6})$$

which means that the bulk-to-boundary propagator ($\tau = \tau_1 < \tau_2 = \tau_f \rightarrow 0_-$) is defined based on the above bulk-to-bulk propagator. The bulk-to-boundary propagator includes one ‘‘plus-type’’ $G_+(\mathbf{k}, \tau)$ and one ‘‘minus-type’’ $G_-(\mathbf{k}, \tau)$:

$$\tau \bullet \text{---} \square = G_+(\mathbf{k}, \tau), \quad (\text{C.7a})$$

$$\tau \circ \text{---} \square = G_-(\mathbf{k}, \tau), \quad (\text{C.7b})$$

where the square at one end of the propagator indicates its boundary point ($\tau_f \rightarrow 0^-$), and a black dot and a white dot denotes ‘‘plus-type’’ and ‘‘minus-type’’, respectively. In

addition, a shaded dot (often representing a vertex) indicates that the possibilities from both the plus-type and minus-type propagators should be summed up:

$$\tau \text{---} \text{---} \square = G_+(\mathbf{k}, \tau) + G_-(\mathbf{k}, \tau). \quad (\text{C.8})$$

The “plus-type” and “minus-type” bulk-to-boundary propagators take the following forms:

$$G_+(\mathbf{k}, \tau) = \frac{H^2}{2k^3} [1 - ik(\tau - \tau_f) + k^2 \tau \tau_f] e^{ik(\tau - \tau_f)} \simeq \frac{H^2}{2k^3} [1 - ik\tau] e^{ik\tau}, \quad (\text{C.9a})$$

$$G_-(\mathbf{k}, \tau) = \frac{H^2}{2k^3} [1 + ik(\tau - \tau_f) + k^2 \tau \tau_f] e^{-ik(\tau - \tau_f)} \simeq \frac{H^2}{2k^3} [1 + ik\tau] e^{-ik\tau}. \quad (\text{C.9b})$$

D Probability Distribution Function of Higgs Field

For the sake of convenience, we abbreviate the Hubble parameter during the inflation H_{inf} as H , namely, $H_{\text{inf}} = H$. A scalar field $\phi(\mathbf{x}, t)$ with only one degree of freedom can be represented as the mode functions of long wavelength part $\phi_L(\mathbf{x}, t)$ and short wavelength part $\phi_S(\mathbf{x}, t)$:

$$\begin{aligned} \phi(\mathbf{x}, t) &= \phi_L(\mathbf{x}, t) + \phi_S(\mathbf{x}, t) \\ &= \phi_L(\mathbf{x}, t) + \int \frac{d^3k}{(2\pi)^3} \theta(k - \epsilon a(t)H) \left[a_{\mathbf{k}} \phi_{\mathbf{k}}(t) e^{-i\mathbf{k}\cdot\mathbf{x}} + a_{\mathbf{k}}^\dagger \phi_{\mathbf{k}}^*(t) e^{i\mathbf{k}\cdot\mathbf{x}} \right]. \end{aligned} \quad (\text{D.1})$$

The short-wavelength modes $\phi_{\mathbf{k}}(t)$ are initially sub-horizon. Over the time, as the universe expands, these modes are stretched and eventually cross the physical cutoff $\epsilon a(t)H$, transitioning into the super-horizon modes ϕ_L . The super-horizon modes ϕ_L can be effectively treated as a classical stochastic field, obeying the Langevin equation:

$$\dot{\phi}_L(\mathbf{x}, t) = -\frac{1}{3H} \frac{\partial V}{\partial \phi_L} + f(\mathbf{x}, t). \quad (\text{D.2})$$

In addition to the force from the potential of the field, the long-wavelength modes are also driven by an effective stochastic “force” f , which is generated by freezing out the short-wavelength modes,

$$f(\mathbf{x}, t) = \int \frac{d^3k}{(2\pi)^3} \delta(k - \epsilon a(t)H) \epsilon a(t) H^2 \left[a_{\mathbf{k}} \phi_{\mathbf{k}}(t) e^{-i\mathbf{k}\cdot\mathbf{x}} + a_{\mathbf{k}}^\dagger \phi_{\mathbf{k}}^*(t) e^{i\mathbf{k}\cdot\mathbf{x}} \right]. \quad (\text{D.3})$$

In order to obtain the Fokker-Planck equation for the one-point probability distribution function, we should derive the two-point correlation function of the stochastic “force” f . For this, we could derive the following relation for a canonical massless field $\phi_{\mathbf{k}}$ in the late-time limit:

$$\begin{aligned} &\left\langle \left(a_{\mathbf{k}_1} \phi_{\mathbf{k}_1}(t_1) e^{-i\mathbf{k}_1 \cdot \mathbf{x}_1} + a_{\mathbf{k}_1}^\dagger \phi_{\mathbf{k}_1}^*(t_1) e^{i\mathbf{k}_1 \cdot \mathbf{x}_1} \right) \left(a_{\mathbf{k}_2} \phi_{\mathbf{k}_2}(t_2) e^{-i\mathbf{k}_2 \cdot \mathbf{x}_2} + a_{\mathbf{k}_2}^\dagger \phi_{\mathbf{k}_2}^*(t_2) e^{i\mathbf{k}_2 \cdot \mathbf{x}_2} \right) \right\rangle \\ &= (2\pi)^3 \delta^3(\mathbf{k}_1 - \mathbf{k}_2) e^{i\mathbf{k}_1 \cdot \mathbf{x}_{12}} \frac{H^2}{2k_1^3}. \end{aligned} \quad (\text{D.4})$$

Then, we can derive the two-point correlation function of f as follows:

$$\begin{aligned}
\langle f(\mathbf{x}_1, t_1) f(\mathbf{x}_2, t_2) \rangle &= \int \frac{d^3 k_1}{(2\pi)^3} \left(\prod_{i=1}^2 \delta(k_1 - \epsilon a(t_i) H) \epsilon a(t_i) H^2 \right) \frac{H^2}{2k_1^3} e^{i\mathbf{k}_1 \cdot \mathbf{x}_{12}} \\
&= \frac{1}{4\pi^2} \int_0^{+\infty} dk_1 \left(\prod_{i=1}^2 \delta(k_1 - \epsilon a(t_i) H) \epsilon a(t_i) H^2 \right) \frac{H^2}{k_1} j_0(k_1 x_{12}) \\
&= \frac{H^5 \epsilon j_0(\epsilon a(t_1) H x_{12}) \delta(\epsilon a(t_1) H - \epsilon a(t_2) H)}{4\pi^2 a(t_1)} \prod_{i=1}^2 a(t_i),
\end{aligned} \tag{D.5}$$

where $\mathbf{x}_{12} = \mathbf{x}_1 - \mathbf{x}_2$, $x_{12} = |\mathbf{x}_{12}|$, and $j_0(z) = (\sin z)/z$ is the spherical Bessel function of zeroth order. Using the property of the delta function, we can simplify the above formula for the two-point correlation function of the stochastic ‘‘force’’:

$$\langle f(\mathbf{x}_1, t_1) f(\mathbf{x}_2, t_2) \rangle = \frac{H^3}{4\pi^2} j_0(\epsilon a(t_1) H x_{12}) \delta(t_1 - t_2). \tag{D.6}$$

If we take the one-point limit $\mathbf{x}_2 \rightarrow \mathbf{x}_1$ in the position space with $j_0(\epsilon a H x_{12}) \rightarrow 1$, the one-point probability distribution function for the field ϕ obeys the Fokker-Planck equation:

$$\frac{\partial \rho(\phi, t)}{\partial t} = \frac{1}{3H} \left\{ \rho(\phi, t) \frac{\partial^2 V(\phi)}{\partial \phi^2} + \frac{\partial V(\phi)}{\partial \phi} \frac{\partial \rho(\phi, t)}{\partial \phi} \right\} + \frac{H^3}{8\pi^2} \frac{\partial^2 \rho(\phi, t)}{\partial \phi^2}, \tag{D.7}$$

To solve Eq.(D.7), we decompose the solution $\rho(\phi, t)$ in terms of the eigenfunctions $\{\Psi_n\}$ with eigenvalues $\{\Lambda_n\}$:

$$\rho(\phi, t) = e^{-v} \sum_{n=0}^{\infty} a_n \Psi_n(\phi) e^{-\Lambda_n(t-t_0)}, \tag{D.8}$$

where v is defined as

$$v(\phi) = \frac{4\pi^2 V(\phi)}{3H^4}, \tag{D.9}$$

and the coefficients a_n could be given by the initial condition of $\rho(t=t_0)$:

$$a_n = \int d\phi \rho(\phi, t_0) e^{v(\phi)} \Psi_n(\phi). \tag{D.10}$$

Then, we can derive the corresponding equation for the eigenfunctions Ψ_n and eigenvalues Λ_n . We may rewrite Eq.(D.8) as $\rho(\phi, t) = \sum_{n=0}^{\infty} \rho_n(\phi, t)$ with

$$\rho_n \equiv e^{-v} \Psi_n a_n e^{-\Lambda_n(t-t_0)}. \tag{D.11}$$

Using the following equations,

$$\frac{\partial \rho_n}{\partial \phi} = \left(-\frac{\partial v}{\partial \phi} \Psi_n + \frac{\partial \Psi_n}{\partial \phi} \right) a_n e^{-v-\Lambda_n(t-t_0)}, \tag{D.12}$$

$$\frac{\partial^2 \rho_n}{\partial \phi^2} = \left\{ \left[\left(\frac{\partial v}{\partial \phi} \right)^2 - \frac{\partial^2 v}{\partial \phi^2} \right] \Psi_n - 2 \frac{\partial v}{\partial \phi} \frac{\partial \Psi_n}{\partial \phi} + \frac{\partial^2 \Psi_n}{\partial \phi^2} \right\} a_n e^{-v-\Lambda_n(t-t_0)}, \tag{D.13}$$

we find that the eigenfunctions Ψ_n and eigenvalues Λ_n satisfy the following equation:

$$\left[\frac{\partial^2}{\partial \phi^2} + \frac{\partial^2 v}{\partial \phi^2} - \left(\frac{\partial v}{\partial \phi} \right)^2 \right] \Psi_n(\phi) = -\frac{8\pi^2}{H^3} \Lambda_n \Psi_n(\phi), \quad (\text{D.14})$$

which is a typical Sturm–Liouville equation. Thus, we find that all of eigenvalues Λ_n are non-negative and the eigenfunctions $\Psi_n(\phi)$ are orthonormal functions,

$$\int_{-\infty}^{+\infty} d\phi \Psi_n(\phi) \Psi_{n'}(\phi) = \delta_{n,n'}. \quad (\text{D.15})$$

They satisfy the completeness condition,

$$\sum_n \Psi_n(\phi) \Psi_n(\phi_0) = \delta(\phi - \phi_0). \quad (\text{D.16})$$

There is a special eigenfunction with the eigenvalue $\Lambda_0 = 0$,

$$\Psi_0(\phi) = N_0 e^{-v(\phi)}, \quad (\text{D.17})$$

Thus, Eq.(D.8) may be represented as

$$\rho(\phi, t) = \Psi_0(\phi) \sum_{n=0}^{\infty} b_n \Psi_n(\phi) e^{-\Lambda_n(t-t_0)}, \quad (\text{D.18})$$

where coefficients b_n are also the normalization factors analogous to a_n , defined as $b_n \equiv a_n/N_0$. If the inflation lasts long enough, the system quickly approaches its equilibrium state. The only term that remains in the above summation is $\Psi_0(\phi)$ with $\Lambda_0 = 0$. Thus, the equilibrium probability distribution $\rho_{1\text{eq}}$ is derived as

$$\rho_{1\text{eq}}(\phi) = \Psi_0(\phi)^2 = N_0^2 \exp\left(-\frac{8\pi^2 V(\phi)}{3H^4}\right), \quad (\text{D.19})$$

where the equilibrium probability distribution satisfies the normalization condition,

$$\int d\phi \rho_{1\text{eq}}(\phi) = 1. \quad (\text{D.20})$$

References

- [1] P. Minkowski, $\mu \rightarrow e\gamma$ at a Rate of One Out of 10^9 Muon Decays? Phys. Lett. B 67 (1977) 421–428.
- [2] M. Gell-Mann, P. Ramond, and R. Slansky, *Complex Spinors and Unified Theories*, Conf. Proc. C 790927 (1979) 315; T. Yanagida, *Horizontal gauge symmetry and masses of neutrinos*, Conf. Proc. C 7902131 (1979) 95; S. L. Glashow, *The Future of Elementary Particle Physics*, NATO Sci. Ser. B 61 (1980) 687; R. N. Mohapatra and G. Senjanovic, *Neutrino Mass and Spontaneous Parity Nonconservation*, Phys. Rev. Lett. 44 (1980) 912; J. Schechter and J. W. F. Valle, *Neutrino Masses in $SU(2) \times U(1)$ Theories*, Phys. Rev. D 22 (1980) 2227.
- [3] Planck Collaboration, N. Aghanim et al., *Planck 2018 Results I. Overview and the cosmological legacy of Planck*, Astron. Astrophys. 641 (2020) A1, [[arXiv:1807.06205](#) [astro-ph.CO]].
- [4] Planck Collaboration, Y. Akrami et al., *Planck 2018 Results IX. Constraints on primordial non-Gaussianity*, Astron. Astrophys. 641 (2020) A9, [[arXiv:1905.05697](#) [astro-ph.CO]].
- [5] Planck Collaboration, Y. Akrami et al., *Planck 2018 Results X. Constraints on inflation*, Astron. Astrophys. 641 (2020) A10, [[arXiv:1807.06211](#) [astro-ph.CO]].
- [6] J. M. Maldacena, *Non-Gaussian features of primordial fluctuations in single field inflationary models*, JHEP 05 (2003) 013, [[astro-ph/0210603](#)].
- [7] For a review, P. D. Meerburg et al., *Primordial Non-Gaussianity*, Bull. Am. Astron. Soc. 51 (2019) 107 [[arXiv:1903.04409](#) [astro-ph.CO]].
- [8] N. Arkani-Hamed and J. Maldacena, *Cosmological Collider Physics*, [[arXiv:1503.08043](#) [hep-th]].
- [9] X. Chen, *Primordial Non-Gaussianities from Inflation Models*, *Advances in Astronomy* 2010 (2010) 638979 [[arXiv:1002.1416](#) [astro-ph.CO]]; X. Chen and Y. Wang, *Quasi-Single Field Inflation and Non-Gaussianities*, JCAP 04 (2010) 027 [[arXiv:0911.3380](#) [hep-th]].
- [10] H. Lee, D. Baumann, and G. L. Pimentel, *Non-Gaussianity as a particle detector*, JHEP 12 (2016) 040 [[arXiv:1607.03735](#) [hep-th]].
- [11] X. Chen, Y. Wang, and Z. Z. Xianyu, *Loop corrections to standard model fields in inflation*, JHEP 08 (2016) 051 [[arXiv:1604.07841](#) [hep-th]]; X. Chen, Y. Wang, and Z. Z. Xianyu, *Standard model mass spectrum in inflationary universe*, JHEP 04 (2017) 058 [[arXiv:1612.08122](#) [hep-th]].
- [12] J. B. Munoz, Y. Ali-Haimoud, and M. Kamionkowski, *Primordial non-gaussianity from the bispectrum of 21-cm fluctuations in the dark ages*, Phys. Rev. D 92 (2015) no.8, 083508 [[arXiv:1506.04152](#) [astro-ph.CO]].
- [13] P. D. Meerburg, M. Munchmeyer, J. B. Munoz, and X. Chen, *Prospects for Cosmological Collider Physics*, JCAP 03 (2017) 050 [[arXiv:1610.06559](#) [astro-ph.CO]].
- [14] P. D. Meerburg et al., *Primordial Non-Gaussianity*, Bull. Am. Astron. Soc. 51 (2019) no.3, 107 [[arXiv:1903.04409](#) [astro-ph.CO]].
- [15] M. Fukugita and T. Yanagida, *Baryogenesis Without Grand Unification*, Phys. Lett. B 174 (1986) 45.

- [16] G. Dvali, A. Gruzinov, and M. Zaldarriaga, *A new mechanism for generating density perturbations from inflation*, Phys. Rev. D 69 (2004) 023505, [[arXiv:astro-ph/0303591](#)].
- [17] S. Lu, Y. Wang and Z. Z. Xianyu, *A cosmological Higgs collider*, JHEP 02 (2020) 011 [[arXiv:1907.07390](#) [hep-th]].
- [18] D. Buttazzo, G. Degrassi, P. P. Giardino, G. F. Giudice, F. Sala, A. Salvio, A. Strumia, *Investigating the near-criticality of the Higgs boson*, JHEP 08 (2012) 098 [[arXiv:1205.6497](#) [hep-ph]].
- [19] S. Navas *et al.* [Particle Data Group], *Top Quark*, Phys. Rev. D 110 (2024) 030001.
- [20] H.-J. He and Z.-Z. Xianyu, *Extending Higgs Inflation with TeV Scale New Physics*, JCAP 10 (2014) 019 [[arXiv:1405.7331](#)].
- [21] V. Gorbenko and L. Senatore, $\lambda\phi^4$ in dS , [[arXiv:1911.00022](#) [hep-th]].
- [22] M. Baumgart and R. Sundrum, *De Sitter Diagrammar and the Resummation of Time*, JHEP 07 (2020) 119, [[arXiv:1912.09502](#) [hep-th]].
- [23] S. Cespedes, A.-C. Davis, and D.-G. Wang, *On the IR divergences in de Sitter space: loops, resummation and the semi-classical wavefunction*, JHEP 04 (2024) 004, [[arXiv:2311.17990](#) [hep-th]].
- [24] A. Starobinsky, *Dynamics of phase transition in the new inflationary universe scenario and generation of perturbations*, Phys. Lett. B 117 (1982), no.3, 175–178.
- [25] A. A. Starobinsky and J. Yokoyama, *Equilibrium state of a self-interacting scalar field in the de Sitter background*, Phys. Rev. D 50 (1994), no.10, 6357–6368 [[arXiv:astro-ph/9407016](#)].
- [26] R. B. Guenther and J. W. Lee, *Sturm-Liouville Problems: Theory and Numerical Implementation*, CRC Press, Taylor and Francis Group, 2018.
- [27] K. Freese, J. A. Frieman and A. V. Olinto, *Natural inflation with pseudo-Nambu-Goldstone bosons*, Phys. Rev. Lett. 65 (1990), 3233-3236.
- [28] E. Silverstein and A. Westphal, *Monodromy in the CMB: Gravity Waves and String Inflation*, Phys. Rev. D 78 (2008) 106003 [[arXiv:0803.3085](#) [hep-th]].
- [29] L. McAllister, E. Silverstein and A. Westphal, *Gravity Waves and Linear Inflation from Axion Monodromy*, Phys. Rev. D 82 (2010) 046003 [[arXiv:0808.0706](#) [hep-th]].
- [30] A. Karam, T. Markkanen, L. Marzola, S. Nurmi, M. Raidal, and A. Rajantie, *Novel mechanism for primordial perturbations in minimal extensions of the Standard Model*, JHEP 11 (2020) 153, [[arXiv:2006.14404](#) [hep-ph]].
- [31] X. Chen, Y. Wang, and Z.-Z. Xianyu, *Neutrino Signatures in Primordial Non-Gaussianities*, JHEP 09 (2018) 022, [[arXiv:1805.02656](#) [hep-ph]].
- [32] A. Hook, J. Huang, and D. Racco, *Searches for other vacua. Part II. A new Higgstory at the cosmological collider*, JHEP 01 (2020) 105, [[arXiv:1907.10624](#) [hep-ph]].
- [33] A. A. Starobinsky, *Dynamics of Phase Transition in the New Inflationary Universe Scenario and Generation of Perturbations*, Phys. Lett. B 117 (1982) 175–178.
- [34] D. S. Salopek and J. R. Bond, *nonlinear evolution of long wavelength metric fluctuations in inflationary models*, Phys. Rev. D 42 (1990) 3936–3962.
- [35] G. L. Comer, N. Deruelle, D. Langlois, and J. Parry, *Growth or decay of cosmological inhomogeneities as a function of their equation of state*, Phys. Rev. D 49 (1994) 2759–2768.

- [36] M. Sasaki and E. D. Stewart, *A General analytic formula for the spectral index of the density perturbations produced during inflation*, Prog. Theor. Phys. 95 (1996) 71–78 [[astro-ph/9507001](#)].
- [37] M. Sasaki and T. Tanaka, *Superhorizon scale dynamics of multiscalar inflation*, Prog. Theor. Phys. 99 (1998) 763–782, [[gr-qc/9801017](#)].
- [38] D. Wands, K. A. Malik, D. H. Lyth, and A. R. Liddle, *A New approach to the evolution of cosmological perturbations on large scales*, Phys. Rev. D 62 (2000) 043527 [[astro-ph/0003278](#)].
- [39] D. H. Lyth and D. Wands, *Conserved cosmological perturbations*, Phys. Rev. D 68 (2003) 103515 [[astro-ph/0306498](#)].
- [40] G. I. Rigopoulos and E. P. S. Shellard, *The separate universe approach and the evolution of nonlinear superhorizon cosmological perturbations*, Phys. Rev. D 68 (2003) 123518 [[astro-ph/0306620](#)].
- [41] D. H. Lyth, K. A. Malik, and M. Sasaki, *A General proof of the conservation of the curvature perturbation*, JCAP 05 (2005) 004 [[astro-ph/0411220](#)].
- [42] T. Suyama and S. Yokoyama, JCAP **06** (2013), 018 doi:10.1088/1475-7516/2013/06/018 [[arXiv:1303.1254](#) [[astro-ph.CO](#)]].
- [43] D. Wands, *Local non-Gaussianity from inflation*, Class. Quant. Grav. 27 (2010) 124002 [[arXiv:1004.0818](#) [[astro-ph.CO](#)]].
- [44] K. Ichikawa, T. Suyama, T. Takahashi, and M. Yamaguchi, *Primordial Curvature Fluctuation and Its Non-Gaussianity in Models with Modulated Reheating*, Phys. Rev. D 78 (2008) 063545 [[arXiv:0807.3988](#) [[astro-ph](#)]].
- [45] A. De Simone, H. Perrier, and A. Riotto, *Non-Gaussianities from the Standard Model Higgs*, JCAP 01 (2013) 037 [[arXiv:1210.6618](#)].
- [46] A. Karam, T. Markkanen, L. Marzola, S. Nurmi, M. Raidal, and A. Rajantie, *Higgs-like spectator field as the origin of structure*, Eur. Phys. J. C 81 (2021) 620, no.7, [[arXiv:2103.02569](#) [[hep-ph](#)]].
- [47] A. Litsa, K. Freese, E. I. Sfakianakis, P. Stengel, and L. Visinelli, *Primordial non-Gaussianity from the effects of the Standard Model Higgs during reheating after inflation*, JCAP 03 (2023) 033 [[arXiv:2011.11649](#)].
- [48] Planck Collaboration, N. Aghanim et al., *Planck 2018 Results. VI. Cosmological Parameters*, Astron. Astrophys. 641 (2020) A6 [[arXiv:1807.06209](#) [[astro-ph.CO](#)]]; Astron. Astrophys. 652 (2021) C4 (Erratum).
- [49] S. Weinberg, *Quantum contributions to cosmological correlations*, Phys. Rev. D 72 (2005) 043514 [[hep-th/0506236](#)]; *Quantum contributions to cosmological correlations II. can these corrections become large?* Phys. Rev. D 74 (2006) 023508 [[hep-th/0605244](#)].
- [50] X. Chen, Y. Wang, and Z. Z. Xianyu, *Schwinger-Keldysh diagrammatics for primordial perturbations*, JCAP 12 (2017) 006 [[arXiv:1703.10166](#)].
- [51] S. Antusch, J. Kersten, M. Lindner, and M. Ratz, *Running neutrino masses, mixings and CP phases: Analytical results and phenomenological consequences*, Nucl. Phys. B 674 (2003) 401 [[arXiv:hep-ph/0305273](#)].

- [52] H.-J. He and F.-R. Yin, *Common Origin of μ - τ and CP Breaking in Neutrino Seesaw, Baryon Asymmetry, and Hidden Flavor Symmetry*, Phys. Rev. D 84 (2011) 033009 [[arXiv:1104.2654](#)]; S.-F. Ge, H.-J. He, F.-R. Yin, *Common origin of soft μ - τ and CP breaking in neutrino seesaw and the origin of matter*, JCAP 05 (2010) 017 [[arXiv:1001.0940](#)]
- [53] S. Alam et al. [eBOSS Collaboration], *Completed SDSS-IV extended Baryon Oscillation Spectroscopic Survey: Cosmological implications from two decades of spectroscopic surveys at the Apache Point Observatory*, Phys. Rev. D 103 (2021) 083533, no.8 [[arXiv:2007.08991](#)].
- [54] T. M. C. Abbott et al. [DES Collaboration], *Dark Energy Survey Year 3 results: Cosmological constraints from galaxy clustering and weak lensing*, Phys. Rev. D 105 (2022) 023520, no.2 [[arXiv:2105.13549](#)].
- [55] A. Aghamousa et al. [DESI Collaboration], *The DESI Experiment Part I: Science, Targeting, and Survey Design*, [[arXiv:1611.00036](#) [astro-ph.IM]].
- [56] K. Abazajian, et al. [CMB-S4 Collaboration], *CMB-S4 Science Case, Reference Design, and Project Plan*, [[arXiv:1907.04473](#) [astro-ph.IM]].
- [57] L. Amendola, et al. [Euclid Collaboration], *Cosmology and fundamental physics with the Euclid satellite*, Living Rev. Rel. 21 (2018) no.1 [[arXiv:1606.00180](#) [astro-ph.CO]].
- [58] O. Dore et al. [SPHEREx Collaboration], *Cosmology with the SPHEREx All-Sky Spectral Survey*, [[arXiv:1412.4872](#) [astro-ph.CO]].
- [59] R. Acciarri et al. [LSST Science Collaboration], *LSST Science Book, Version 2.0*, [[arXiv:0912.0201](#)].
- [60] A. Weltman, et al. *Fundamental physics with the Square Kilometre Array*, Publ. Astron. Soc. Austral. 37 (2020), [[arXiv:1810.02680](#) [astro-ph.CO]].
- [61] F. An et al. [JUNO Collaboration], *Neutrino Physics with JUNO*, J. Phys. G 43 (2016) no.3, 030401 [[arXiv:1507.05613](#)].
- [62] R. Acciarri et al. [DUNE Collaboration], *Long-Baseline Neutrino Facility (LBNF) and Deep Underground Neutrino Experiment (DUNE): Conceptual Design Report, Volume 1: The LBNF and DUNE Projects*, [[arXiv:1601.05471](#)].
- [63] M. J. Dolinski, A. W. P. Poon, and W. Rodejohann, *Neutrinoless Double-Beta Decay: Status and Prospects*, Ann. Rev. Nucl. Part. Sci. 69 (2019) 219-251 [[arXiv:1902.04097](#) [nucl-ex]].
- [64] C. Han, H.-J. He, L. Song, and J. You, *Cosmological Signatures of Neutrino Seesaw*, [[arXiv:2412.21045](#)].